Dullius, Darlene J.; Borges, Victor Gabriel; Vargas, Renzo; Gusk, Caitlin; Tonkoski, Reinaldo; Melo, Joel D.; Kasmaei, Mahdi Pourakbari

Analysis of Financial Penalties for Low Power Factor in Distribution Systems with High Penetration of Photovoltaics

Published in:
IEEE Access

DOI:
10.1109/ACCESS.2024.3493379

Published: 01/01/2024

Document Version
Publisher's PDF, also known as Version of record

IEEE Access
Multidisciplinary | Rapid Review | Open Access Journal

Received 17 September 2024, accepted 31 October 2024, date of publication 7 November 2024, date of current version 22 November 2024.

Digital Object Identifier 10.1109/ACCESS.2024.3493379

RESEARCH ARTICLE

Analysis of Financial Penalties for Low Power Factor in Distribution Systems With High Penetration of Photovoltaics

DARLENE J. DULLIUS[1], VICTOR GABRIEL BORGES[1], RENZO VARGAS[2], CAITLIN GUSK[3], REINALDO TONKOSKI[3,4], (Senior Member, IEEE), JOEL D. MELO[1], (Senior Member, IEEE), AND MAHDI POURAKBARI KASMAEI[5], (Senior Member, IEEE)

[1]Center for Engineering, Modeling and Applied Social Sciences, Federal University of ABC, Santo André 09210-580, Brazil
[2]Institute of Energy and Environment, University of São Paulo, São Paulo 05508-010, Brazil
[3]Department of Electrical and Computer Engineering, College of Engineering, The University of Maine (UMaine), Orono, ME 04469, USA
[4]Department of Energy and Process Engineering, Technical University of Munich (TUM), 80333 Munich, Germany
[5]Department of Electrical Engineering and Automation, Aalto University, 02150 Espoo, Finland

Corresponding author: Darlene J. Dullius (darlene.dullius@ufabc.edu.br)

This work was supported in part by the Coordination for the Improvement of Higher Education Personnel (CAPES)—Finance Code 001 under Grant 88887.709682/2022-00 and Grant 88887.692379/2022-00, in part by Brazilian National Council for Scientific and Technological Development (CNPq) under Grant 407244/2023-9 and 408898/2021-6, in part by São Paulo Research Foundation (FAPESP) under Grant #2021/08832-1 and Grant #2023/17658-0, and in part by the National Institute of Science and Technology of Electric Energy-Brazil (INCT-INERGE).

ABSTRACT Several countries have encouraged the installation of photovoltaic (PV) systems in urban areas to contribute to the decarbonization goals of the electric power system. At the same time, consumers have adopted PV systems to reduce their electricity bills. While grid-following PV inverters offset active power demand, they can decrease the power factor at the point of interconnection with the grid, subsequently leading to financial penalties imposed by distribution utilities. Additionally, utilities must maintain power factor values above a predefined threshold to maintain acceptable levels of power losses at the transmission level. This paper examines low power factor penalty schemes for distribution utilities and consumers with PV systems. In such an analysis, an optimization approach is used to minimize the costs of penalties associated with low power factor during a consumer's billing period. This approach makes it possible to reduce the number of low power factor penalties, thus reducing the amount of electricity bills to be paid by consumers. The decision variable in this context is the power factor of the PV inverters. A case study is presented that considers the financial penalties in a city in the metropolitan area of Sao Paulo, Brazil, with various levels of PV penetration in the distribution system. The results show that while the penalties for consumers are low, distribution utilities would incur more significant penalties or require additional investments to maintain the power factor at the values imposed by electric transmission companies. This analysis aims to help regulatory agencies evaluate penalty schemes to reduce electrical losses in the distribution system.

INDEX TERMS PV systems, power factor, financial penalties schemes, power distribution systems.

I. INTRODUCTION

In recent years, the installation of photovoltaic (PV) systems has experienced growth due to a variety of factors. These factors, including the rise in demand for clean energy to meet decarbonization goals [1], federal policies like the solar investment tax credit [2], and efforts to decrease acquisition costs [3], contribute to the transition toward more sustainable energy sources. For example, in 2023, PV systems in Brazil generated 41.343 GWh [4] as a result of a 19% increase in installed power compared to 2022 [4]. However, this high penetration of PV systems leads to new challenges in ensuring electric grid stability and adequate power quality [5].

The associate editor coordinating the review of this manuscript and approving it for publication was Zhehan Yi.

High penetration of PV can produce undesirable effects at the medium (MV) and low voltage (LV) grids, as discussed in [6] and [7]. For instance, high penetration of PV systems in distribution networks can increase voltage levels along long feeders [8] as well as cause changes in the power factor [9].

During periods of high solar irradiation, the PV system can meet most of the consumers' active energy demands, reducing electricity costs. This reduction is because only active power is billed by distribution utilities and there are no penalties for low power factor. In general, penalty schemes for low power factors are applied to consumers to ensure that they meet most of their reactive power demands locally and that power losses in distribution networks are not increased due to the delivery of the consumers' reactive demand [10]. However, when photovoltaic generation meets or compensates only for active power demand, it can reduce the power factor measurement at the point of connection to the grid, called power factor degradation [11]. This degradation does not increase power losses in distribution networks but can lead to penalties. These penalties may occur when the power factor recorded at the point of common coupling (PCC) is below the minimum requirement of the distribution utilities [12]. Fig. 1 shows that in the absence of solar power, both active and reactive powers are exclusively consumed by the load from the grid supply. The meter, in this scenario, computes a higher power factor due to the predominance of active power from the grid. When a PV system is introduced, and the PV inverter operates at the unity power factor, it results in no contribution to reactive power. However, the inverter does contribute to active power, thereby reducing the active power consumption from the grid. The meter, installed at the grid connection point, calculates the power factor based on the reduced active power value, while the reactive power remains unchanged. Consequently, this leads to a reduction in the power factor at the PCC [13].

This paper analyzes whether low power factor penalty schemes are sufficient to encourage consumers with PV Systems to maintain power factor values above those imposed on regulatory agencies. The outcomes of this study aim to help identify the need for changes in penalty schemes in areas with high levels of PV penetration. The main contributions of this paper are:

- Analyzing the effectiveness of low power factor penalty schemes to encourage consumers to maintain their power factor within the minimum required value;
- Developing an optimization model for adjusting the power factor of consumers' PV inverters that reduces penalties for low power factor in their electricity billing without the need to install new reactive power compensation equipment;
- Analyzing the impact of the low power factor on the PCC and the substation located on the border between transmission and distribution.

The remainder of this work is as organized as follows. Section II presents how the apparent degradation of the power

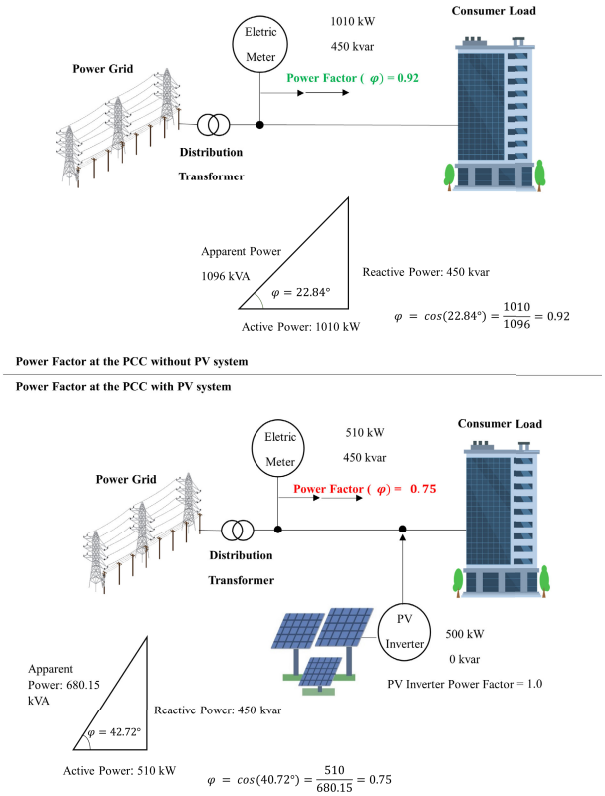

FIGURE 1. Example of PV Integration impact on power factor at the PCC.

factor in the PCC occurs due to the installation of PV systems compensating only for the consumers' active power demand. Section III shows a brief review of penalty schemes imposed on consumers and utilities in different countries. Section IV describes how adjusting the power factor of PV inverters can improve the power factor of the consumer at the PCC with the grid. A formulation is also presented in Section IV to minimize the daily billing of consumers by adjusting the power factor of PV inverters to avoid penalties related to low power factor. Section V provides observations and discussions regarding real distribution feeders for a Brazilian city in the metropolitan area of Sao Paulo. Finally, the conclusions and recommendations for utilities are presented in Section VI.

II. APPARENT POWER FACTOR DEGRADATION DUE TO PV SYSTEMS

In this work, we present a mathematical model that focuses on consumers with PV systems connected to the MV grid, particularly when their PV inverters are connected to the LV network. The nominal apparent power of the load is represented as $S_{nominal} = P_t + jQ_t$, where P_t and Q_t denote the active and reactive power consumed during the time interval t in a measurement period of electricity billing, respectively. Similarly, the nominal apparent power of the PV inverter is given as $S_{nominal_{PV}} = P_{PV_t} + jQ_{PV_t}$, where P_{PV_t} and Q_{PV_t} represent the active and reactive power injected by

the PV inverter at the time interval t, respectively. To analyze the impact of the operation of the PV inverter on the utility's measurements, we define $P'_t = P_t - P_{PV_t}$ as the total active power measured by the distribution utility during the time interval t, and $Q'_t = Q_t - Q_{PV_t}$ as the total reactive power measured by the utility during the time interval t. The power factor measured at the PCC during the interval t is σ_t and is found using (1).

$$\sigma_t = \frac{P'_t}{\sqrt{(P'^2_t + Q'^2_t)}} \tag{1}$$

In this work, we consider that the controls available on the PV inverter will not allow their operation to exceed the maximum capacity of the PV inverter ($S_{nominal_{PV}}$) at any interval t. Adjustments of the PV inverter power factor (σ_{PV_t}) for values different than one result in Q_{PV_t} values other than zero, resulting in a decrease in the P_{PV_t} value that compensates for the consumer's active power demand. Thus, when a PV inverter operates with a unity power factor ($\sigma_{PV_t} = 1$), as the photovoltaic plant's production increases, the PV system will achieve higher compensation for active power demand. However, this operational mode, which aims to take advantage of the entire $S_{nominal_{PV}}$, may result in an apparent degradation of the power factor measured at the PCC as the value of P'_t decreases compared to the value of Q'_t.

Power factor analysis in PCC is typically performed hourly by the distribution utility, while data is measured at 15-minute intervals by the utility. In past decades, in which we had a unidirectional power flow, from the substation to meet consumer demand, utilities interpreted a low power factor as an increase in reactive power demand that increased the power losses of their distribution networks [10]. The penalty schemes sought to ensure consumers compensate locally for their reactive power demand. Thus, a low power factor at the PCC resulted in economic penalties if it fell below a limit established by the system regulator [14]. The applied penalty schemes are discussed in Section III.

III. LOW POWER FACTOR PENALTY SCHEMES

Typically, the electricity bill for MV consumers includes prices for active power, demand rates, and costs for reactive power due to penalties from the low power factor [15]. The penalties for power factor are imposed when the power factor at the PCC falls below the minimum value required by the distribution utilities [16].

The penalties for low power factor can be applied to both consumers and distribution utilities. Each country establishes a range or a single threshold value so that no penalties are applied. In Victoria, power factor limits vary depending on the supply voltage and consumer demand. For instance, for a supply voltage ranging from 6.6 kV to 22 kV and a demand between 100 kVA and 2 MVA, the minimum power factor can be 0.85 lagging or 0.9 leading [17]. Tasmania also follows these regulations, adopting the values specified for Victoria for the equivalent supply voltage and demand conditions [18]. In the UK, the distribution system operator (DSO) is responsible for imposing penalties when the power factor drops below 0.95 [16]. In Malaysia, a power factor surcharge is imposed if the power factor is less than 0.90 for electricity supplies of 132 kV and above or less than 0.85 for electricity supplies below 132 kV. For electricity supplies below 132 kV, a 1. 5% surcharge on the current bill is imposed for every 0.01 decrease in the power factor below 0.85. In addition, a 3% surcharge of the current bill is imposed for every 0.01 decrease in the power factor below 0.75 [19].

These calculations are based on the difference between the customer's actual power factor and the specified power factor levels (0.85 and 0.75). The surcharge is then applied to the total customer's bill, which includes charges for energy consumed (kWh), energy capacity (kW) and imbalance cost pass-through (ICPT) [20]. ICPT is a mechanism within the incentive-based regulatory framework that enables a utility, such as TNB, to adjust electricity rates every six months [19]. In Slovenia, power factor charges are applied to both loads and DSOs when the power factor falls below 0.95, regardless of the type of deviation (inductive or capacitive). These charges remain uniform without differentiating between voltage levels, specific time intervals (including 15-minute segments), or geographic locations. These charges are applied to all, encompassing all connection points for a given user. The fixed rate is 3.34 € per megavolt-ampere reactive hour (Mvarh) whenever the power factor falls below the 0.95 threshold [21]. In Iceland, the required average power factor is 0.9 at the out-feed for DSOs and for power-intensive users at each point of delivery [21].

The rules governing the injected and consumed reactive power in Bulgaria differ from those in other countries. The penalty for consuming or transmitting reactive power is 10% of the wholesale price of the active power, while the penalty for injecting reactive power is 100% of the wholesale price of the active power. The reactive power consumed, for which the penalty is imposed on the consumer, is calculated according to (2) [21].

$$EQP_t = EQ_t - (0.49 \times EP_t) \tag{2}$$

In (2), EQP_t represents the amount of reactive power that incurs a penalty during the time interval t, EQ_t represents the reactive power consumed during the time interval t, 0.49 is the coefficient adopted by [21] to achieve a power factor of 0.9, and EP_t is the active power consumed during the same interval. The same penalty calculation method applies to distribution utilities, as shown in (2). However, for these utilities, the variables EQ_t and EP_t are substituted with the quantities of reactive power delivered from the transmission network to the distribution network and the active power produced during the time interval t, respectively, which is generally 15 minutes [21]. The regulatory agencies measure these quantities in the border region between the transmission and distribution systems.

In Brazil, the reactive energy charges (REC) are applied to consumers connected to MV supplied with a voltage lower

than 69 kV. The mechanism for REC is described in [15] for consumers, the power factor must be between 0.92 and 1.0, whether capacitive or inductive [22]. Meanwhile, for distribution utilities, the penalty of low power factor (PLPF) is generally calculated using the net operating income or the estimated value for energy production. To determine the cost of the penalty, data from the twelve months before the infraction is analyzed, as described in [23]. Infractions related to low power factor for the calculation basis of the penalty may reach 0.5% of the net operating income (NOI) or estimated value of energy production. For simplicity, in this work, we assume that PLPF applied to distribution utilities represents 0.5% of NOI. The calculation of PLPF for a day is presented in (3).

$$PLFP = \frac{0.005\ NOI}{365} \tag{3}$$

Taking into account the NOI, the penalties applied to companies can be much higher than those applied to consumers. In addition, a low power factor at the PCC or the boundary areas can have a negative impact on the electrical system. From a financial standpoint, these penalties can lead to decisions regarding investments in new equipment and changes to the network infrastructure [24]. This means that keeping the power factor above the minimum value required by the regulatory agency should be a concern for both consumers and distribution utilities.

IV. THE USED METHODOLOGY TO ANALYZE THE PENALTY SCHEME FOR LOW POWER FACTOR

This section presents the methodology for analyzing the low power factor penalty scheme for MV consumers with PV systems and distribution utilities. In such an analysis, we consider that consumers wish to decrease their energy bills without installing reactive compensation equipment. In this way, we formulate an optimization model, minimizing the number of infractions due to low power factor values, considering the operating voltage restrictions of consumer equipment and its demand balance. In the methodology used, this model is applied to each consumer in the analysis, adjusting each PV inverter's power factor. After obtaining the power factor of PV inverters of all consumers that receive energy from a distribution substation located on the border with the transmission system, the next stage of the methodology is to execute power flow software to determine the power factor that the distribution utility will measure.

The first stage of the methodology is illustrated in Fig. 2. In this stage, the PV inverters for each consumer in the analysis are initially set to operate at a unity power factor. Subsequently, the presence of REC charges on consumers' electricity bills is identified, along with the PLFP for the distribution utility. If REC charges are found, the PV inverters are adjusted by solving an optimization model that aims to minimize the consumer's electricity bills by reducing penalties for low power factor. In this work, the optimization is performed using the flower pollination algorithm (FPA),

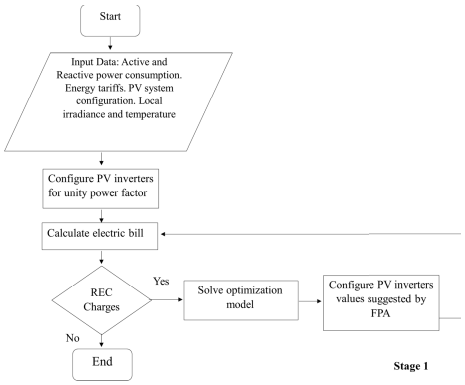

FIGURE 2. First stage flowchart of the performed methodology.

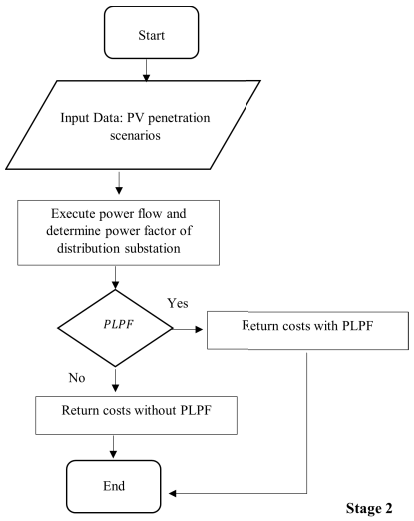

FIGURE 3. Second stage flowchart of the performed methodology.

a computational intelligence technique with a minimum power factor requirement of 0.92, as mandated by the current regulations in the country under study. The FPA was chosen due to its few parameters, which are easily calibrated by the DSO, and its fast convergence, as described in [25]. After implementing the FPA's suggested adjustments, the penalties for REC charges are recalculated to determine the new REC values.

In the appendix, results from alternative optimization techniques, such as Particle Swarm Optimization (PSO) and the Fibonacci Search Algorithm, are also presented. For the PSO, both the number of particles and iterations are set to 100, with an inertia weight of 0.5 and cognitive and social coefficients of 1.5 each. For the Fibonacci method, the number of iterations is 10, with a tolerance and precision of 10^{-4}. In both cases, the search space boundaries range from 0.9 to 1.0. Although a detailed comparison of these techniques is beyond the scope of this paper, the appendix illustrates that different methods can also be applied to adjust the power factor.

The appendix further examines how penalties for low power factor are impacted when the minimum required power factor at the PCC is altered. This analysis considers threshold values of 0.85, 0.9, 0.92, and 0.95.

It is important to note that for the minimum required power factor values of 0.85 and 0.9, there are cases where no penalties are detected. Consequently, the algorithm makes no adjustments, and no results are presented in the appendix for these scenarios.

In the second stage of the methodology, as presented in Fig. 3, power flow software is employed to determine the power factor at the distribution substation. Several PV penetration scenarios are then considered to analyze their impact on the operational variables of the distribution network. For each scenario, the costs of penalties for low power factor (PLPF) to the distribution utility are determined. In constructing these scenarios, it is assumed that other consumers without photovoltaic systems connected to the same feeder have similar consumption characteristics.

A. MATHEMATICAL FORMULATION TO REDUCE PENALTIES FOR LOW POWER FACTOR ON CONSUMERS' ELECTRICITY BILLS

This section provides detailed information on modeling penalties for low power factors on consumers' electricity bills with photovoltaic systems considered in the performed methodology. The optimization model's objective function, F, is presented in (4), aiming to minimize the expenses associated with the electricity bill. It explicitly targets adjustments to the power factor of the PV inverter to lessen charges that arise from a low power factor within a specified period, REC_t. Thus, solving the optimization model minimizes electricity expenses by reducing the penalties applied for low power factor. In this paper, the day-ahead calculation is considered.

$$minF = \sum_{p\in\Omega_p}\sum_{t\in\Omega_t}(AEEC_{t,p}TE_{t,p}) + (AEEC_{t,p}TUSD_{t,p}) + REC_t \quad (4)$$

In (4), Ω_t represents the total number of periods on the electricity billing day. Ω_p is the total number of tariff stations. Many distribution systems utilize two tariff stations, applied by utilities, to distinguish between peak and off-peak times. The peak hour, is when the energy consumption in the distribution system is at its highest. The remaining periods of the day constitute the off-peak times. The tariff stations are refered as p. $TE_{t,p}$ is the tariff in US$/kWh applied for energy use during the tariff station p and the time interval t. $TUSD_{t,p}$ is the tariff in US$/kWh for the use of distribution system during the tariff station p and the time interval t. REC_t is the value corresponding to the reactive electric charges during a billing period at the interval t. REC_t is calculated hourly for a one-day billing period using (5), and will show up in the electricity bill only when low power factor values are identified.

$$REC_t = \sum_{p\in\Omega_p}\sum_{t\in\Omega_t} AEEC_{t,p}\left(\frac{\sigma_{ref}}{\sigma_t} - 1\right) TE_{t,p} \quad (5)$$

In (5), σ_{ref} represents the minimum power factor established by the regulatory agency. A possible mechanism to reduce the REC_t is to adjust the power factor of the PV inverters (σ_{PV_t}). In this work, this adjustment is by finding a solution to the optimization model using the FPA algorithm whose objective function (4) and considering the limits of the values presented in (6).

$$\sigma_{\min} \le \sigma_{PV_t} \le \sigma_{\max} \quad \forall t \in \Omega_t \quad (6)$$

In (7), the PV reactive power injection is presented. $Q_{PV,t}$ represents the injection of PV inverter reactive power at a time interval t. This injection of reactive power relies on the inverter's active power injection at the time interval ($P_{PV,t}$) and on the power factor value adjusted in the PV inverters.

$$Q_{PV,t} = P_{PV,t}\tan\left(\cos^{-1}(\sigma_{PV_t})\right) \quad \forall t \in \Omega_t \quad (7)$$

The apparent power limit of the PV inverter, $S_{nominal_{PV}}$, is shown in (8).

$$(P_{PV,t})^2 + (Q_{PV,t})^2 \le \quad (S_{\text{nominal}_{PV}})^2 \quad \forall t \in \Omega_t \quad (8)$$

In this work, the analysis is carried out considering an offline approach, using forecasts of demand and generation to estimate the energy billed the following day in each consumer unit. Furthermore, in cases where a consumer has more than one PV system and to ensure that the power factor adjustment of the PV inverters can meet the maximum value of permitted losses, the proposal considers the execution of a power flow in the internal network of the consumer unit. The power flow balance equations for this network with distributed generation are presented in (9) and (10).

$$P^G_{k,t} - P^D_{k,t} = V_{k,t} \times \sum_{m\in\Omega_m}\sum_{t\in\Omega_t} V_{m,t} \times (G_{km}\cos\theta_{km,t} + B_{km}\sin\theta_{km,t}) \quad (9)$$

$$Q^G_{k,t} - Q^D_{k,t} = V_{k,t} \times \sum_{m\in\Omega_m}\sum_{t\in\Omega_t} V_{m,t} \times (G_{km}\sin\theta_{km,t} + B_{km}\cos\theta_{km,t}) \quad (10)$$

where $P^G_{k,t}$ and $Q^G_{k,t}$ are the active and reactive power generated at the bus k during time interval t, respectively. $P^D_{k,t}$ and $Q^D_{k,t}$ are the active and reactive power demanded at the bus k during time interval t, respectively. Ω_m is the set of buses adjacent to the bus k. $V_{k,t}$ is the voltage at the bus k during time interval t, and $V_{m,t}$ is the voltage at the bus m during the time interval t. G_{km} is the conductance between buses k and m, while B_{km} is the susceptance between buses k and m. $\theta_{km,t}$ is the angle of voltage difference between buses k and m at time interval t. The power flow is performed, considering the voltage limits presented in (11).

$$V_{\min} \le V_{k,t} \le V_{\max} \quad \forall k \in \Omega_K, \forall t \in \Omega_t \quad (11)$$

In (11), $V_{k,t}$ represents the voltage at the node k during a time interval t. V_{min} and V_{max} denote the required minimum and maximum voltage values, respectively. The subsequent section outlines the steps involved in adjusting the power factor of PV inverters (σ_{PV_t}) using the FPA algorithm.

B. APPLICATION OF THE FLOWER POLLINATION ALGORITHM TO MINIMIZE THE NUMBER OF PENALTIES DUE TO LOW POWER FACTOR

The FPA is a metaheuristic optimization algorithm that can be used to determine the optimal power factor configuration of PV inverters to correct the power factor at the PCC. It has several advantages over other optimization algorithms, including a small number of parameters to be calibrated, fast convergence time, high-quality results for nonlinear systems with continuous decision variables [26], robustness, scalability, and adaptability to different problem domains. FPA has been used in a variety of electrical systems applications, such as [27]. In these applications, it has consistently produced good results compared to other optimization methods.

It is a metaheuristic technique based on the process of flower pollination. The process of pollination can be divided into two main categories: biotic and abiotic. Approximately 90% of pollination occurs biotically, where pollen from a plant is transported to another plant by insects or animals. Abiotic pollination does not require pollinating agents and is then a consequence of winds and diffusion in the water [28]. The main characteristics of the pollination algorithm are as follows.

1) Biotic and cross-pollination are considered global pollination processes with pollinating agents whose trajectory is described by Lévy's flights.
2) Abiotic pollination and self-pollination are considered local pollination.
3) Flower constancy can be considered since the probability of reproduction is proportional to the similarity of the two flowers involved.
4) Local and global pollination are controlled by a probability of change $pc \in [0, 1]$. Due to physical proximity and other factors such as wind, local pollination can have a significant fraction pc in overall pollination activities.

In order to simplify the pollination process, the FPA technique assumes that each plant has a single flower and that each flower can produce only one pollen gamete. However, there is no need to distinguish the gamete, pollen, flower, plant, or the solution to the problem. This simplification means that the solution x_i is valid for both the flower and the gamete [28].

The FPA considers that in the global pollination process, pollen from flowers is carried by pollinating agents such as insects and that pollen can travel over long distances because insects can fly and move over large areas. This ensures the best pollination and production, which is represented as g_* [28]. The first premise and flower constancy can be mathematically described in (12).

$$[x_i^{t+1} = x_i^t + L(x_i^t - g_*)] \tag{12}$$

where x_i^t represent the pollen i or solution vector x_i at iteration t, and g_* represents the incumbent solution. The parameter L denotes the pollination strength, which is equivalent to the step size. Insects are known to move over large distances with multiple step distances, and this characteristic can be effectively simulated using Lévy flights [28]. On the other hand, local pollination is described in (13).

$$[x_i^{t+1} = x_i^t + \epsilon(x_j^t - x_k^t)] \tag{13}$$

where x_j^t and x_k^t represent pollen from different flowers of the same plant species, which represents neighborhood-limited breeding behavior. Mathematically, if x_j^t and x_k^t are of the same species or selected from the same population, this describes a local random path if we consider ϵ as a uniform distribution that takes values between 0 and 1.

Most flower pollination activities can occur on either a local or global scale. In practice, flowers in proximity or adjacent plots are more likely to be pollinated by local pollen. Therefore, the criterion of the probability of change or proximity is used to generate alternating cycles between common global and intensive local pollination [28].

In both global and local search methods, a solution vector, x_i, is utilized, as detailed in the mathematical model presented in Section IV. The dimensions of this vector correspond to the number of inverters connected to the consumer's grid. Each element in x_i is representative of the power factor of an inverter, and these elements are continuous variables within a specified search range.

The quality of a solution is determined based on the value of the objective function (4). A lower value of the objective function signifies a higher-quality solution. Among all the solutions in the population, the one with the highest quality is designated as the incumbent solution, g_*.

In this work, the implementation of the FPA algorithm necessitates distinct power factor adjustments for each hour within the generation interval spanning from 6 a.m. to 6 p.m. This approach is employed when identifying instances of low power factor infractions during the specified time frame. To execute the algorithm, it is necessary to specify an initial range with the maximum and minimum values that can be adjusted (a,b), the number of flowers ($n_{flowers}$), switching probability for local and global search (pc), the number of iterations (k), as well as the necessary parameters for the pollination strength ($\Gamma(\lambda)$) defined by Lévy's flight.

To analyze how the adjustments made by the FPA algorithm in the PV inverters of the consumers can modify the power factors in the substation, penetration scenarios of PV generators are considered in the next section.

C. PV GENERATION SCENARIOS

In the second stage of the methodology, the distribution utilities' power network must be modeled to execute load flow software considering the adjustment of the power factor of the PV inverters found in the previous stage. Power flow software, such as OpenDSS [29] and Matpower [30], can be used. In this work, we model the power distribution network in Matpower tool [30]. The Python language was used through a package that communicates between Matpower and Python called Pypower [31] to simulate operating conditions in the distribution network. The performed methodology considers the power factor values at the substation with a resolution of one hour for one day, totaling 24 hourly values.

In specialized literature, different levels of penetration and their effects have been analyzed [32]. At [33] levels of 5%, 10%, 30-50% the effects on voltage regulation are analyzed. In turn, [34] considers 5 different levels of 10%, 20%, 30%, 40% and 50% and analyzes different impacts on the network. This approach allowed us to capture the various power factor effects in the distribution substation at different DG penetration levels.

V. RESULTS OF THE APPLICATION OF THE PERFORMED METHODOLOGY

This section presents the application of the two stages explained in Section IV for three feeders of an electrical substation in a city in the metropolitan region of Sao Paulo. It's important to highlight that this active power compensation was non-existent prior to the implementation of PV systems. As a result of this absence of such compensation, both consumers were not subjected to penalties for a low power factor (p_f). However, penalties appear after the installation of PV systems, justifying the need to adjust the power factor of the inverters.

Initially, information about the case study will be presented, showing the load curves of two consumers with high compensation values for their active power demand. Then, the power factor adjustments to minimize bill charges for infractions are determined. After conducting these adjustments and the invoice amount, the low power factor infractions in the substation will be shown, considering different PV penetration scenarios. Finally, discussions about the penalty values for consumers and the distribution company will be presented.

A. CASE STUDY

This section provides detailed information about the case study. Two consumers with different consumption profiles were considered. Both are assumed to have similar PV system specifications. After analyzing the consumers, the impact on the power factor in the distribution substation is observed.

1) CONSUMPTION PROFILE OF THE CONSUMERS

The first consumer is a university. The University has a peak active power demand from 12 a.m. to 3 p.m., and reactive power demand is almost continuous throughout the day. This behavior is shown in Fig. 4. It is important to note that the consumption may vary according to the school period, with low active power consumption on weekends.

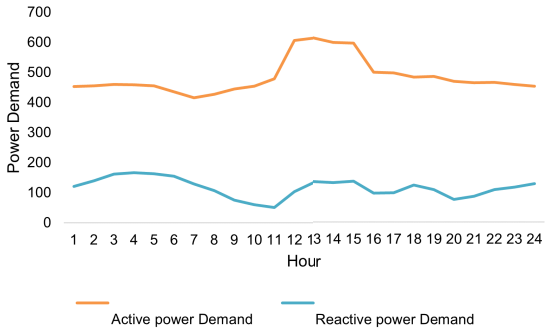

FIGURE 4. Typical consumption profile federal university of ABC.

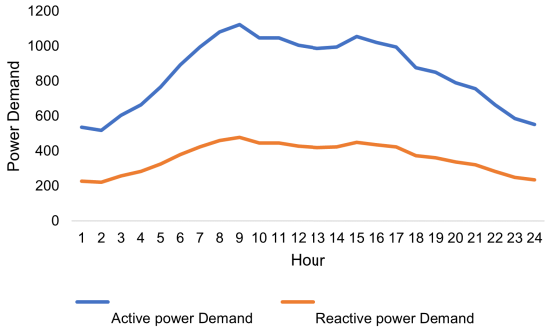

FIGURE 5. Typical consumption profile industrial consumer.

The second consumer is an industry with a higher demand for active and reactive power compared to the University. The consumption is distributed throughout the day, starting from the first hours of sunlight, as shown in Fig. 5. Since this is an industrial consumer, there are no significant variations in consumption throughout the year.

2) TOPOLOGY OF THE ELECTRICAL NETWORK OF CONSUMERS WITH PV SYSTEMS

Fig. 6 shows the considered topology with PV systems in each consumer. OpenDSS [29] was used to model the electrical network and the consumer's load curve, while Python was used to implement the FPA algorithm. The consumers are connected to a nominal voltage of 13.8 kV, and their internal LV network operates at a nominal voltage of 0.22 kV. The minimum and maximum voltage limits are 0.95 p.u. and 1.05 p.u.

A total of nine PV systems have been installed at five different points on the LV side of the grid in each consumer unit, as shown in Fig. 6. The AC generation capacity of inverters 1, 3, 4, 5, 6, 7, and 8 is 33 kVA. Inverters 2 and 9 have a capacity of 55 kVA. Due to technical requirements,

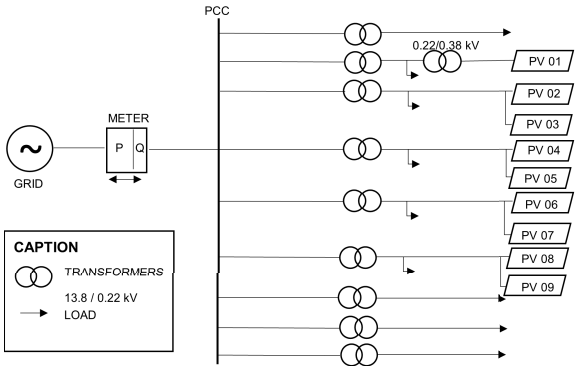

FIGURE 6. Single-line diagram of the interconnection of the PV Systems in the distribution system.

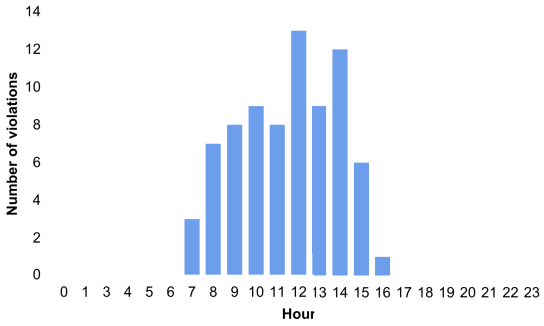

FIGURE 7. Number of infractions due to low p_f assuming unity power factor on PV inverters in UFABC.

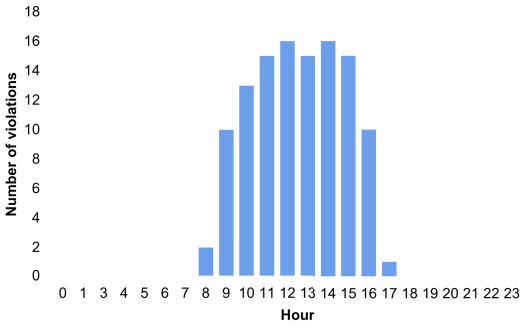

FIGURE 8. Number of infractions due to low p_f assuming unity power factor on PV inverters in industrial consumer.

the inverters are limited to operate within a range of a leading power factor of 0.90 and a lagging power factor of 0.90.

A typical day during the period from 2018 to 2021, specifically from October to December, was selected for analysis. These months were chosen because they were identified as the period during which the highest number of infractions occurred. This observation can be attributed to the concurrent rise in irradiance within the region, coupled with alterations in load patterns, particularly during the year-end holiday season.

To better understand the impact of these factors, 18 different scenarios were constructed. These scenarios vary based on combinations of different irradiance levels and load patterns measured during the period. Each scenario represents a unique combination of these variables, allowing for the analysis of a wide range of possible conditions and their effects on the system. These scenarios were applied to two different consumer profiles (University and Industrial) to assess their impacts comprehensively. The power factor analysis is performed hourly at the PCC, following the recommendations presented in [15]. Consequently, the information is gathered in one-hour intervals, resulting in a total of 24 measurements. The predefined power factor threshold to avoid penalties is set at 0.92, according to [15].

The performance of the proposed approach is evaluated using real data from the Federal University of ABC (UFABC) in Santo Andre, Brazil, and a typical industrial consumer. The single-line diagram of the grid interconnection of the PV Systems for both is presented in Fig. 6. The simulation experiments were conducted using OpenDSS with Python [35], Matpower [30] and Pypower [31] on a computer with a 3.6 GHz Intel(R) Xeon(R) E-2246G processor and 32 GB of RAM. Furthermore, for this analysis, 1 US dollar is considered equivalent to 5.20 reals (R$), based on the future dollar projection [36].

B. INITIAL SOLUTION: SETTING UNITY POWER FACTOR ON PV INVERTERS

In this section, all PV inverters are assumed to operate at a unity power factor. This assumption is made to achieve maximum active power compensation. Fig. 7 and Fig. 8 show the number of infractions due to low power factor when all PV inverters are assumed to operate with a unity power factor. In the industrial profile, most infractions occur from 9 a.m. to 2 p.m. In both profiles, critical low values are registered during peak PV system production times. It is important to note that reactive power compensation from PV inverters could correct the power factor at the PCC. In each of the PV penetration scenarios, the adjustment values of the power factor of the PV inverters to minimize the consumers electricity bill will be considered as input data.

C. RESULTS USING FPA TO ADJUST THE POWER FACTOR OF PV INVERTERS

Since the adjustment FPA algorithm is only executed in the presence of *REC* charges on the electricity bill, it is necessary first to define peak and off-peak hours. These hours are used to calculate the electricity bill. Accordingly, peak hours are defined in the interval of 5:45 p.m. to 08:30 p.m while the remaining hours are considered off-peak. If low power factor infractions are found within this period, the FPA algorithm is executed. Table 1 presents the parameters used to execute the FPA algorithm in each run.

After setting the parameters, the algorithm for adjusting the power factor of the PV inverters is applied. For each hour of the day where there are infractions due to low p_f values, an adjustment setting is made. In this case study, only

TABLE 1. FPA initialization parameters.

$n_{flowers}$	100
a	0.9
b	1.0
k	100
Γ	0.1
Λ	1.5
pc	0.75

infractions occurring within the generation period between 6 a.m. and 6 p.m. are considered.

1) THE ADJUSTED VALUES FOR PV INVERTERS OF THE FEDERAL UNIVERSITY CONSUMER

Fig. 9 illustrates the variation of the adjusted values for each inverter within the 18 scenarios evaluated for a weekday in the months of October through December, between 2018 and 2021. Due to the intermittency of the solar resource, the power factor adjustment values are directly related to the variations in irradiance and temperature observed during the day [37]. Therefore, obtaining a range of values that can be adjusted provides information on the maximum variation expected. For this reason, the results are presented as confidence intervals [38]. For small sample sizes, typically 25 or fewer, the confidence interval is calculated as [39]:

$$I_{upper} = \mu - t(n - 1.005) \cdot \psi\sqrt{n} \quad (14)$$

$$I_{lower} = \mu + t(n - 1.005) \cdot \psi\sqrt{n} \quad (15)$$

where μ represents the arithmetic average of the sample, ψ the standard deviation of the sample size (n). The $t(n-1.005)$ value is obtained from the t distribution table [39]. With n equal to 18, $t(n - 1.005)$ is 2.11 for a 95% confidence level [39]. Table 2 presents the confidence intervals obtained for the adjustment values. Fig. 9 and Table 2 show that a single adjustment for all inverters could not lessen the low power factor charges on the consumer's energy bill. Furthermore, we observed that the PV 1 inverter is the one that has the lowest variation in the power factor adjustment of the inverter.

TABLE 2. Power factor adjustment confidence interval of the PV inverters for UFABC.

PV Code	Min. Limit f_p value	Max. Limit f_p value	Mean value
PV 01	0.95	0.97	0.96
PV 02	0.94	0.98	0.96
PV 03	0.93	0.97	0.95
PV 04	0.93	0.97	0.95
PV 05	0.94	0.98	0.96
PV 06	0.93	0.97	0.95
PV 07	0.94	0.97	0.95
PV 08	0.95	0.98	0.96
PV 09	0.94	0.98	0.96

It is worth noting that the maximum and minimum values in the boxplot (as shown in Fig. 9) may differ from those

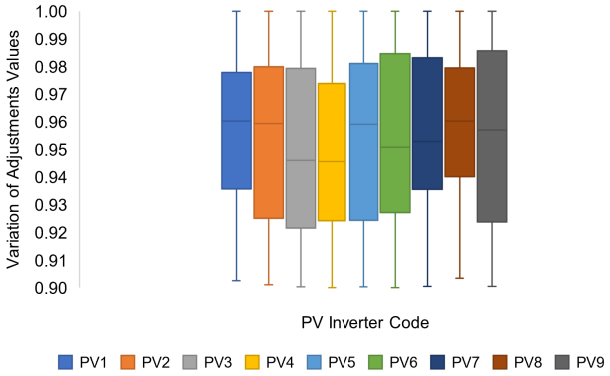

FIGURE 9. Power factor adjustment variation for UFABC.

in the confidence interval presented in Table 2 due to the interquartile calculation and the influence of outliers.

By adopting this adjustment range for each of the PV inverters, the costs with REC decrease. Table 3 shows the penalty values when using the unity power factor and values within the intervals presented in Table 2.

TABLE 3. REC values with unity power factor and FPA adjustment for UFABC.

f_p	Max. Value	Min. Value	Medium Value
Unity	US$ 14.80	US$ 0.21	US$ 4.44
FPA adj.	US$ 1.23	US$ 0.00	US$ 0.22

Employing adjustment values significantly diminishes the REC value. In 80% of the evaluated scenarios, the penalty costs are completely eliminated. This reduction in REC costs subsequently leads to a decrease in the value of the objective function (4). Table 4 presents the values obtained for the electric energy bill when adopting the unity power factor for the PV inverters and using the adjustment values proposed by FPA. Meanwhile, Fig. 10 illustrates the variation of the electric bill and REC costs in both situations.

TABLE 4. Billing values with unity power factor and FPA adjustment for UFABC.

f_p	Max. Value	Min. Value	Medium Value
Unity	US$ 615.33	US$ 419.71	US$ 516.58
FPA adj.	US$ 614.31	US$ 414.71	US$ 513.40

In all the 18 analyzed scenarios, the objective function shown in (4) is reduced. Additionally, the maximum penalty amount, in scenarios where the application of the methodology cannot extinguish the REC, represents approximately 0.26% of the amount that would be paid on the consumer's energy bill. The flower pollination algorithm-based method showed its effectiveness in minimizing the electricity bill by optimizing the power factor of PV inverters. The average computation time required for solving this case is 28.15 minutes.

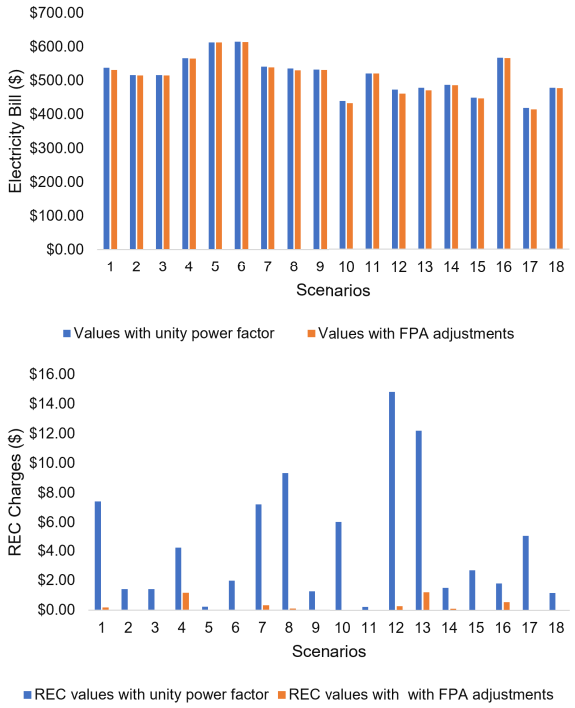

FIGURE 10. Billing and REC costs for UFABC.

2) THE ADJUSTED VALUES FOR PV INVERTERS THE INDUSTRIAL CONSUMER

Fig. 11 shows the variation of the adjusted values for each inverter within 18 scenarios evaluated for a weekday from October between December 2018 and 2021. Table 5 shows the confidence intervals obtained for the adjustment values. This figure and table show slight variations in adjustment among the consumer unit PV inverters. So perhaps a single adjustment for all PV inverters could reduce the low power factor charges bill. However, the methodology performed avoids such charges.

TABLE 5. Power factor adjustment confidence interval of the PV inverters for industrial consumer.

PV Code	Min. Limit f_p value	Max. Limit f_p value	Mean value
PV 01	0.94	0.96	0.95
PV 02	0.94	0.97	0.95
PV 03	0.93	0.96	0.94
PV 04	0.93	0.96	0.95
PV 05	0.94	0.97	0.95
PV 06	0.93	0.96	0.95
PV 07	0.94	0.96	0.95
PV 08	0.94	0.97	0.95
PV 09	0.94	0.97	0.95

Upon adopting the range outlined in Table 5, a variation in REC values is observed. These variations are presented in Table 6

Table 7 presents the maximum, minimum, and average values for the industrial billing costs. Currently, Fig. 12

TABLE 6. REC values with unity power factor and FPA adjustment for industrial consumer.

f_p	Max. Value	Min. Value	Medium Value
Unity	US$ 10.72	US$ 0.45	US$ 6.13
FPA adj.	US$ 0.00	US$ 0.00	US$ 0.00

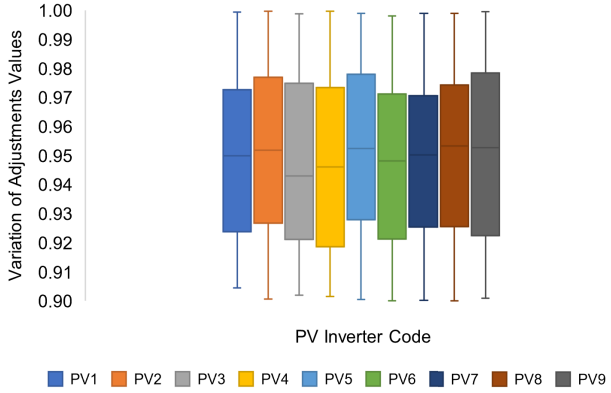

FIGURE 11. Power factor adjustment variation for industrial consumer.

depicts the fluctuations in the electric bill and REC costs under both circumstances.

In all 18 analyzed scenarios, the objective function shown in (4) is reduced. Before the application of the proposal, the maximum penalties represent approximately 0.77% of the amount that would be paid on the consumer's energy bill. With the application of the methodology, the charge bill of low power factor infractions is equal to 0 in all of the scenarios. Consequently, post-adjustment REC costs are not depicted in Fig. 12 The average calculation time required to solve this case is 86.97 minutes.

D. ANALYSIS OF THE POWER FACTOR IN THE SUBSTATION FEEDERS

This section presents the results of the power factor analysis from the feeder perspective.

1) ANALYSIS AFTER APPLYING FPA TO REDUCE CONSUMER'S INFRACTIONS

The impact of PV generation on the substation was also analyzed, observing the same 18 scenarios for both the university and industrial consumers. Without the FPA power factor adjustment, it was identified that in 2 out of the 18 scenarios for the university consumer, the substation power factor decreased. Additionally, it was observed that in these same two scenarios, the FPA algorithm prevented penalties due to the low power factor in the substation by adjusting the power factor of the PV inverters. On the other hand, power factor infractions were not identified for the industrial consumer in the substation.

2) ANALYSIS UNDER DIFFERENT PENETRATION SCENARIOS

To analyze photovoltaic penetration scenarios, the real network of the city of Santo André-SP was modeled, and the

TABLE 7. Billing values with unity power factor and FPA adjustment for industrial consumer.

f_p	Max. Value	Min. Value	Medium Value	$S.D$
Unity	US$ 1512.25	US$ 1397.11	US$ 1447.63	US$ 36.31
FPA adj.	US$ 1511.79	US$ 1389.76	US$ 1443.68	US$ 38.20

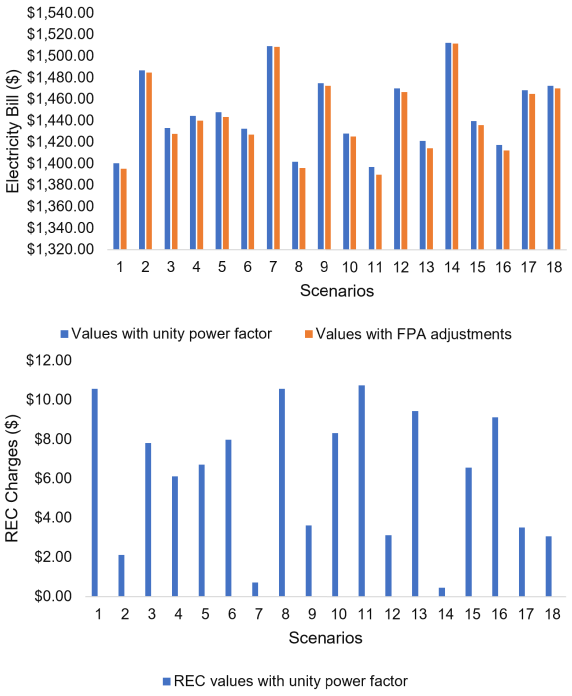

FIGURE 12. Billing and REC costs for the industrial consumer.

power flow was simulated, with the random allocation of PV systems. The power flow calculation determines the hourly time resolution values of active and reactive power at medium voltage substation (HV/MV). Previous studies, such as [40] and [41], have extensively explored the effects of high levels of PV penetration.

To investigate the influence of the increasing integration of DG into the distribution system in analyzing, this study simulates scenarios with varying levels of PV penetration. An initial penetration of 20% was chosen, followed by intermediate levels of 30%, and finally, a high penetration scenario of 50%. The results are shown in Fig. 13, Fig. 14, and Fig. 15. The number of PLPF increases with a growth in PV system penetration.

PV potential was estimated based on [42], using historical time data available from the distribution company. The locations for the placement of PV generators were randomly assigned and distributed across the feeders. The power factor values were recorded at the substation connecting the distribution system with the transmission system to assess whether it was less than some preset limit imposed by regulatory agencies. For instance, values below 0.95 are considered infractions according to the ONS (Brazilian National Electric System Operator) definition.

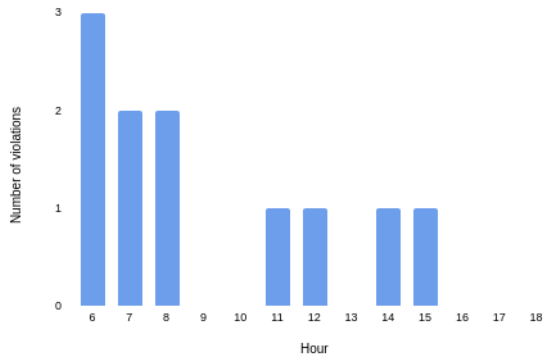

FIGURE 13. Infractions by time with 20% penetration.

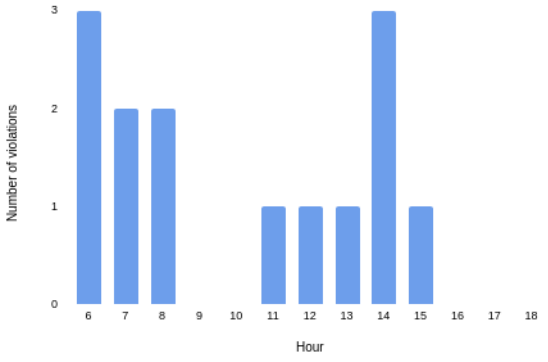

FIGURE 14. Infractions by time with 30% penetration.

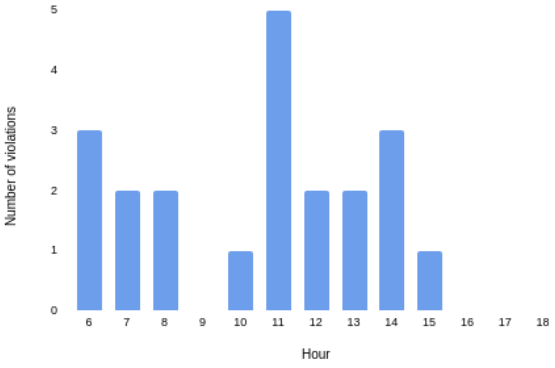

FIGURE 15. Infractions by time with 50% penetration.

Different penetration levels facilitate simulations from lower to higher levels of PV diffusion, allowing analysis of how infractions increase with penetration. After defining the penetration levels, the proposed methodology randomly distributes consumers with identical PV generation characteristics. Subsequently, the PV is allocated to the feeder, and the power flow is simulated to determine the active and reactive power values in the substation.

Using equation (3), fines for each substation power factor infraction amount to 54, 420.63 US$, based on net operating income data from [43]. Additionally, with the profile of the PV generation curve with its respective values of active and reactive power generated over time, the number of

infractions by prosumers and their respective financial value are obtained. By normalizing these values in terms of power, it is possible to infer for the penetration scenarios mentioned above the amounts with penalties that would be charged to them. Table 8 compares PLPF costs for distribution utility at different penetration levels. Meanwhile, Table 9 presents REC costs associated with power factor infraction incurred by consumers. Analyzing electricity bill amounts, reveals that adjusting the power factor and unit factor results in a daily cost reduction of mere cents, which may not sufficiently motivate customers to perform power factor corrections. However, penalties for distribution company, represented by PLPF, are significantly higher than those for consumers, depending on the billing period. These penalty values highlight the need to review penalty calculation methods and to implement mechanisms that encourage consumers to improve their power factor.

TABLE 8. Costs with PLPF in each PV penetration scenario for distribution utility.

Scenario	20%	30%	50%
PLPF ($)	598,626.93	761,888.86	1,142,833.23

TABLE 9. REC costs in each PV penetration scenario for distribution utility.

Scenario	20%	30%	50%
Unity ($)	138,989.06	217,597.1	362,662.16
FPA adj.($)	10,452.65	15,678.92	26,131.56

The values in Table 8 are based on the reference net operating profit presented by [43]. In the scenario with 30% penetration, fines amounted to 27.27%, which is higher than the scenario with 20% penetration. Similarly, with 50% penetration, the increase compared to the 20% scenario was 90.91%.

As utilities incur fines for each infraction, it becomes clear that the impact of low power factor infractions is much greater for distribution companies compared to consumers. In the 50% PV penetration scenario from Table 9, REC costs represent approximately 31.23% before the FPA adjustment and 2.29% after the FPA adjustment, relative to the charges imposed on utilities (PLPF costs). This suggests that in scenarios with higher PV penetration, REC costs for both the UFABC consumer and industrial consumer could represent a significant portion of the charges imposed on utilities. However, if these consumers adjusted their power factor, this portion would be considerably reduced. In other words, the results suggest that higher PV penetration levels combined with specific power factor thresholds can significantly increase financial penalties for both utilities and consumers. Therefore, these findings highlight the importance of optimizing PV penetration and power factor management strategies to mitigate financial risks. Utilities and policymakers should consider these variations when designing incentives and regulations to encourage the adoption of measures that motivate consumers to improve their power factor.

E. ANALYSIS OF POWER LOSSES IN DIFFERENT SCENARIOS

In power distribution systems, power losses stand as a critical concern. They represent an inevitable byproduct of conveying energy from supplying sources to consumer installations. These losses are increasingly emerging as pivotal factors warranting consideration in the planning and operation of electrical distribution networks [44]. Allocations at strategic DG points were used to obtain improvements in terms of active power [45] and reactive power [46]. In contrast to these works, in the present study, the DG was allocated randomly.

An analysis of active power losses and reactive power losses was accomplished in three penetration scenarios: levels of 20%, 30%, and 50%, respectively. This analysis was carried out using the techniques for adjusting the power factor with a unitary value and FPA. Tables 10 and 11 represent the percentage drop in active and reactive power loss values, respectively, compared to the scenario in which there is no DG insertion. Table 10 shows the percentage drop in active power losses for the two adjustment techniques in different penetration scenarios. In turn, Table 11 shows the variation of reactive losses.

TABLE 10. Drop in active power losses with unity power factor and FPA adjustment.

f_p	20%	30%	50%
Unity	-0.07%	-0.12%	-0.18%
FPA adj.	-0.05%	-0.09%	-0.14%

TABLE 11. Drop in reactive power losses with FPA adjustment.

f_p	20%	30%	50%
FPA adj.	-1.31%	-1.82%	-2.63%

The results show that for both adjustment techniques, there was a small reduction in the active power loss values analyzed. In the analysis of reactive power losses, it was observed that the FPA adjustment technique provided a reduction in these losses, leading to drops for the analyzed scenarios of 1.31%, 1.82% and 2.63%, respectively. This represents an advantage over unity adjustment, a technique that does not cause changes in this indicator. The construction of the techniques leads to this result. The FPA adjusts the power factor without keeping the active power fixed. Both the P and Q values are modified, leading to a reduction in reactive power losses in the network.

It is noteworthy to mention that the analyses conducted in this study consider a scenario where there is no supervision of all inverters and the absence of centralized control to mitigate the impact on the substation's power factor. Therefore, each consumer should adjust their PV inverter to avoid penalties for low power factor.

VI. CONCLUSION

This paper presented an approach to reduce the reactive power charging penalty by adjusting the power factor of PV inverters connected to the LV side of the grid in the MV distribution network. The approach has shown reductions in the electricity bill by approximately 0.24% for the university and industrial consumers, with a mean reduction of approximately 0.29%. Additionally, for the university and industrial consumers, the average cost reduction related to low power factor infractions has been over 90%.

The reduction values were compared with those obtained when photovoltaic inverters operate with a unity power factor. In this comparison, we observed that if the low penalty values applied to consumers result, it will not help to cover the high values of financial losses of distribution utilities, making it necessary for regulatory agents to be able to define new penalty schemes for low power factor.

In past decades in which distribution networks did not have DG, an improvement in consumers' power factor brought benefits of reducing power losses in the distribution network, improving the quality of electrical energy, and increasing network capacity. However, in the simulations presented in this work, we can observe that the degradation of the low power factor of consumers with PV does not increase the system's power losses. Energy losses are considered one of the main reasons for applying financial penalties due to the observed degradation in the power factor. In an attempt to avoid such penalties, investments can be made in reactive power compensation equipment, such as capacitor banks.

However, in the literature, it is observed that the improper use of these equipment can lead to issues in regulating network voltage levels. Therefore, regulatory agents must analyze whether it is appropriate to penalize such consumers.

On the other hand, a reduction in the number of infractions by adjusting the power factor of PV inverters contributes to a decrease in the flow of reactive power supplied by the distribution network. The simulations presented in this work show that increasing DG penetration levels can facilitate the reduction of power losses, which leads to the debate on the reason to penalize photovoltaic consumers, even if energy losses do not increase. This growth in DG can lead to network imbalance and infrastructure costs, but the penalty is not justified from the point of view of active and reactive power losses.

The primary goal of this paper was to draw attention to the fact that, from a financial perspective, consumers currently have little motivation to sacrifice part of the active power generated by their photovoltaic systems to avoid penalties for low power factor. Even when penalized, the cost to them is minimal. However, in grids with high photovoltaic penetration, many consumers might incur power factor violations, and if they are not incentivized to correct this parameter, it could negatively impact the power factor at the boundary region. Consequently, the utilities could face substantial penalties.

In future work, we intend to extend the analysis period and explore the impacts of varying irradiance conditions throughout the seasons.

APPENDIX

This section presents the behavior of penalties for the consumer when the minimum required power factor at the PCC is altered and applies the FPA and Fibonacci techniques to perform the adjustment. For the sensitivity analysis, we simulated the behavior of REC penalties by considering σ_{ref} values of 0.85, 0.9, 0.92, and 0.95, reflecting standards observed in other countries. The results for the FPA technique with $\sigma_{ref} = 0.92$ are discussed throughout the article and not in the appendix.

A. FEDERAL UNIVERSITY LOAD PROFILE

This section presents the results for the university load profile (UFABC) using the FPA, PSO and Fibonacci Search and the σ_{ref} values.

1) CONFIDENCE INTERVALS

Tables 12 to 14 present the confidence intervals (C.I) obtained by varying the power factor using the FPA technique.

TABLE 12. FPA - Power factor adjustment C.I of the PV inverters for UFABC ($\sigma_{ref} = 0.85$).

PV Code	Min. Limit f_p value	Max. Limit f_p value	Mean value
PV 01	0.93	0.97	0.95
PV 02	0.93	0.97	0.95
PV 03	0.94	0.98	0.96
PV 04	0.94	0.98	0.96
PV 05	0.93	0.97	0.95
PV 06	0.93	0.97	0.95
PV 07	0.93	0.97	0.95
PV 08	0.93	0.97	0.95
PV 09	0.93	0.97	0.95

TABLE 13. FPA - Power factor adjustment C.I of the PV inverters for UFABC ($\sigma_{ref} = 0.9$).

PV Code	Min. Limit f_p value	Max. Limit f_p value	Mean value
PV 01	0.93	0.97	0.95
PV 02	0.93	0.98	0.96
PV 03	0.94	0.98	0.96
PV 04	0.93	0.97	0.95
PV 05	0.93	0.97	0.95
PV 06	0.93	0.97	0.95
PV 07	0.94	0.98	0.96
PV 08	0.92	0.97	0.95
PV 09	0.93	0.97	0.95

The results obtained using the PSO technique are provided in Tables 16 to 18.

TABLE 14. FPA - Power factor adjustment C.I of the PV inverters for UFABC ($\sigma_{ref} = 0.95$).

PV Code	Min. Limit f_p value	Max. Limit f_p value	Mean value
PV 01	0.94	0.97	0.95
PV 02	0.93	0.96	0.95
PV 03	0.93	0.96	0.95
PV 04	0.93	0.96	0.95
PV 05	0.94	0.97	0.95
PV 06	0.94	0.97	0.95
PV 07	0.93	0.97	0.95
PV 08	0.94	0.97	0.95
PV 09	0.94	0.97	0.95

TABLE 15. PSO - Power factor adjustment C.I of the PV inverters for UFABC ($\sigma_{ref} = 0.85$).

PV Code	Min. Limit f_p value	Max. Limit f_p value	Mean value
PV 01	0.92	0.97	0.95
PV 02	0.93	0.98	0.95
PV 03	0.93	0.98	0.95
PV 04	0.93	0.97	0.95
PV 05	0.92	0.97	0.94
PV 06	0.93	0.97	0.95
PV 07	0.93	0.98	0.95
PV 08	0.93	0.96	0.94
PV 09	0.93	0.98	0.95

TABLE 16. PSO - Power factor adjustment C.I of the PV inverters for UFABC ($\sigma_{ref} = 0.9$).

PV Code	Min. Limit f_p value	Max. Limit f_p value	Mean value
PV 01	0.93	0.97	0.95
PV 02	0.93	0.97	0.95
PV 03	0.93	0.97	0.95
PV 04	0.93	0.97	0.95
PV 05	0.94	0.98	0.96
PV 06	0.93	0.96	0.95
PV 07	0.94	0.98	0.96
PV 08	0.94	0.97	0.96
PV 09	0.94	0.97	0.96

TABLE 17. PSO - Power factor adjustment C.I of the PV inverters for UFABC ($\sigma_{ref} = 0.92$).

PV Code	Min. Limit f_p value	Max. Limit f_p value	Mean value
PV 01	0.93	0.97	0.95
PV 02	0.93	0.96	0.94
PV 03	0.94	0.97	0.95
PV 04	0.93	0.97	0.95
PV 05	0.94	0.97	0.96
PV 06	0.93	0.96	0.94
PV 07	0.93	0.97	0.95
PV 08	0.94	0.97	0.95
PV 09	0.94	0.97	0.96

TABLE 18. PSO - Power factor adjustment confidence interval of the PV inverters for UFABC ($\sigma_{ref} = 0.95$).

PV Code	Min. Limit f_p value	Max. Limit f_p value	Mean value
PV 01	0.93	0.96	0.95
PV 02	0.94	0.97	0.95
PV 03	0.93	0.96	0.95
PV 04	0.93	0.96	0.95
PV 05	0.94	0.97	0.96
PV 06	0.93	0.96	0.95
PV 07	0.93	0.96	0.95
PV 08	0.94	0.96	0.95
PV 09	0.93	0.96	0.95

TABLE 19. Fibonacci - Power factor adjustment confidence interval of the PV inverters for UFABC ($\sigma_{ref} = 0.85$).

PV Code	Min. Limit f_p value	Max. Limit f_p value	Mean value
PV 01	0.90	0.98	0.94
PV 02	0.91	0.99	0.95
PV 03	0.94	1.00	0.97
PV 04	0.97	1.00	0.99
PV 05	0.99	1.00	1.00
PV 06	1.00	1.00	1.00
PV 07	1.00	1.00	1.00
PV 08	1.00	1.00	1.00
PV 09	1.00	1.00	1.00

TABLE 20. Fibonacci - Power factor adjustment C.I of the PV inverters for UFABC ($\sigma_{ref} = 0.9$).

PV Code	Min. Limit f_p value	Max. Limit f_p value	Mean value
PV 01	0.91	0.96	0.93
PV 02	0.92	0.97	0.95
PV 03	0.95	1.00	0.97
PV 04	0.96	1.00	0.98
PV 05	0.99	1.00	1.00
PV 06	0.99	1.00	1.00
PV 07	1.00	1.00	1.00
PV 08	1.00	1.00	1.00
PV 09	1.00	1.00	1.00

TABLE 21. Fibonacci - Power factor adjustment C.I of the PV inverters for UFABC ($\sigma_{ref} = 0.92$).

PV Code	Min. Limit f_p value	Max. Limit f_p value	Mean value
PV 01	0.91	0.96	0.94
PV 02	0.92	0.97	0.94
PV 03	0.95	1.00	0.97
PV 04	0.97	1.00	0.99
PV 05	0.99	1.00	1.00
PV 06	0.99	1.00	1.00
PV 07	1.00	1.00	1.00
PV 08	1.00	1.00	1.00
PV 09	1.00	1.00	1.00

Similarly, Tables 20 to 22 display the results using the Fibonacci Search algorithm.

Regarding the occurrence of power factor violations, it is important to note that for UFABC, changing the minimum power factor threshold had a minimal impact on the number of violations. Specifically, setting the threshold at 0.85 resulted in a maximum of 12 infractions between 6 AM and 6 PM, occurring at noon. The maximum number of infractions increased to 14 for the other power factor thresholds. From the mentioned Tables, is possible to note

TABLE 22. Fibonacci - Power factor adjustment C.I of the PV inverters for UFABC ($\sigma_{ref} = 0.95$).

PV Code	Min. Limit f_p value	Max. Limit f_p value	Mean value
PV 01	0.91	0.96	0.94
PV 02	0.91	0.96	0.94
PV 03	0.94	0.99	0.96
PV 04	0.95	1.00	0.97
PV 05	0.97	1.00	0.99
PV 06	0.98	1.00	0.99
PV 07	0.98	1.00	0.99
PV 08	0.98	1.00	0.99
PV 09	0.98	1.00	1.00

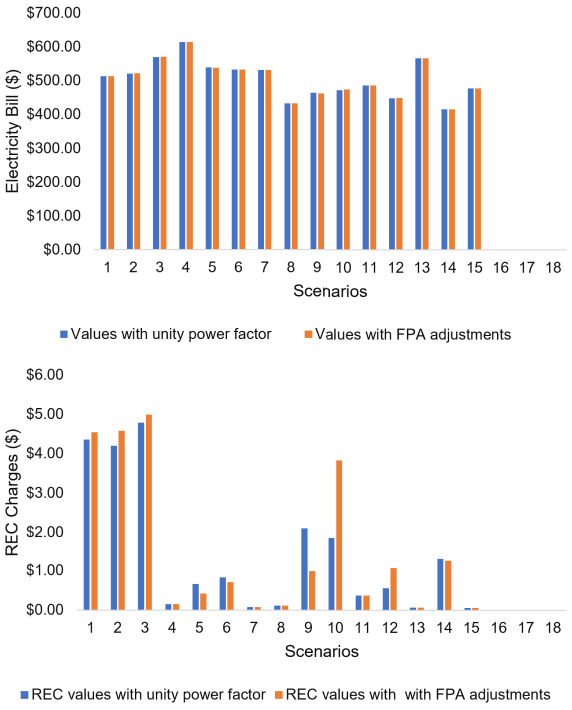

FIGURE 16. FPA - Billing and REC costs for the UFABC consumer ($\sigma_{ref} = 0.85$).

FIGURE 17. FPA - Billing and REC costs for the UFABC consumer($\sigma_{ref} = 0.9$).

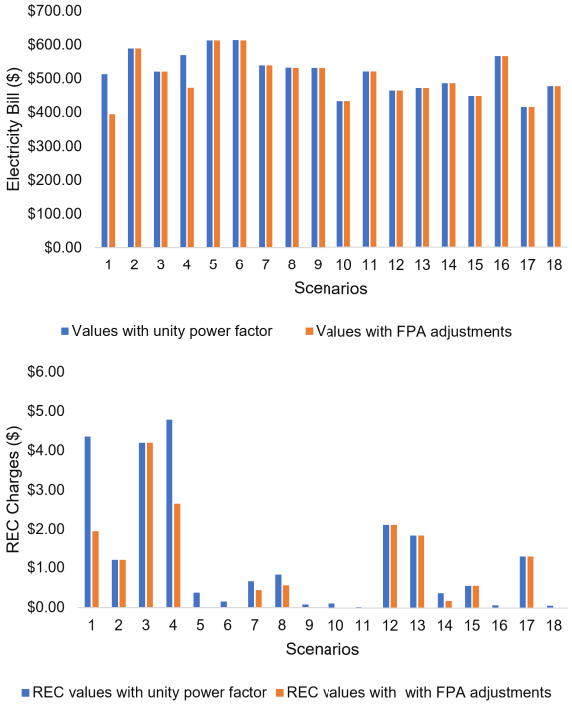

FIGURE 18. FPA - Billing and REC costs for the UFABC consumer($\sigma_{ref} = 0.95$).

that the one-dimensional Fibonacci search algorithm makes minimal adjustments to the power factor values of photovoltaic inverters. For example, with a σ_{ref} of 0.92 inverters 7, 8, and 9 consistently maintained a unity power factor during all time intervals where violations occurred across the 18 analyzed scenarios. In contrast, the FPA algorithm explores a broader search space, adjusting a greater number of PV inverters. As a result, none of the inverters remained at a unity power factor when violations were present. Similarly, the PSO algorithm did not keep any inverter at a unity power factor during periods of violations.

2) BILLING AND REC COSTS

Figs. 16, 17 and 18 present billing and REC costs using the FPA technique.

The FPA technique delivers results that reduce the objective function in all 18 scenarios. The results obtained

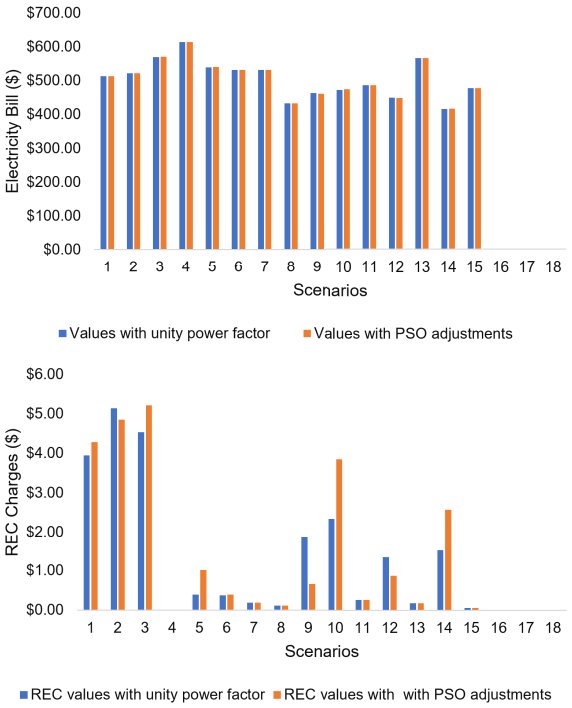

FIGURE 19. PSO - Billing and REC costs for the UFABC consumer ($\sigma_{ref} = 0.85$).

FIGURE 20. PSO - Billing and REC costs for the UFABC consumer($\sigma_{ref} = 0.9$).

using the PSO technique are provided in Fig. 19, 20, 21 and 22.

FIGURE 21. PSO - Billing and REC costs for the UFABC consumer($\sigma_{ref} = 0.92$).

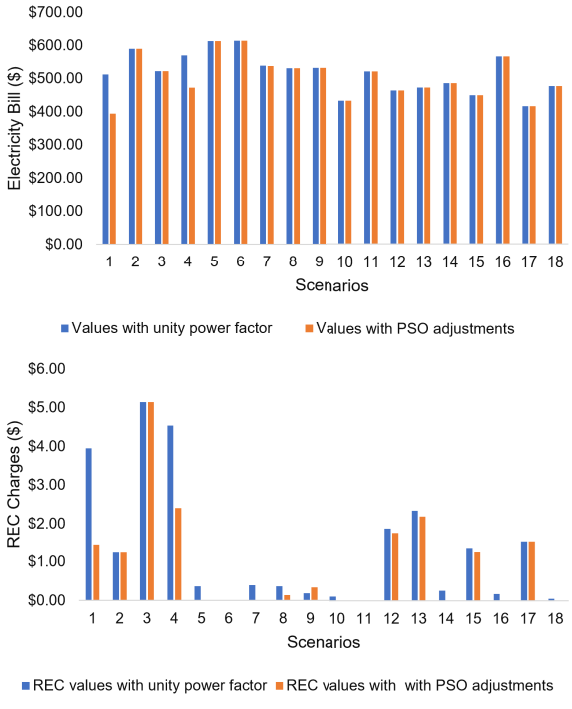

FIGURE 22. PSO - Billing and REC costs for the UFABC consumer($\sigma_{ref} = 0.95$).

For the UFABC curve, with a minimum power factor of 0.92, the PSO algorithm reduces the objective function (the consumer's electricity bill) in 14 out of 18 scenarios.

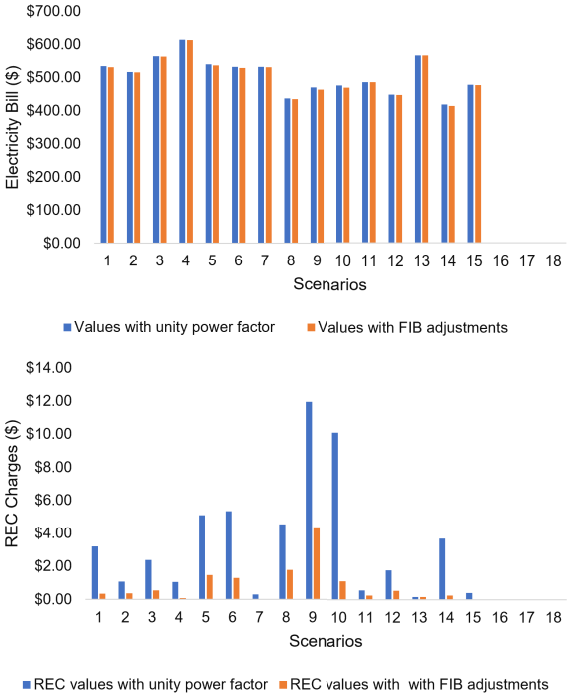

FIGURE 23. Fibonacci - Billing and REC costs for the UFABC consumer ($\sigma_{ref} = 0.85$).

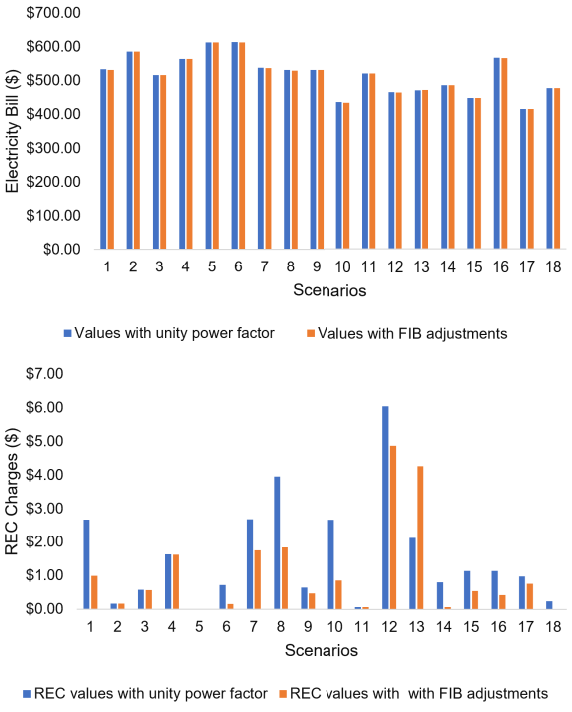

FIGURE 24. Fibonacci - Billing and REC costs for the UFABC consumer($\sigma_{ref} = 0.9$).

Similarly, Figs. 23, 24, 25, 26 display the results using the Fibonacci Search algorithm.

FIGURE 25. Fibonacci - Billing and REC costs for the UFABC consumer($\sigma_{ref} = 0.92$).

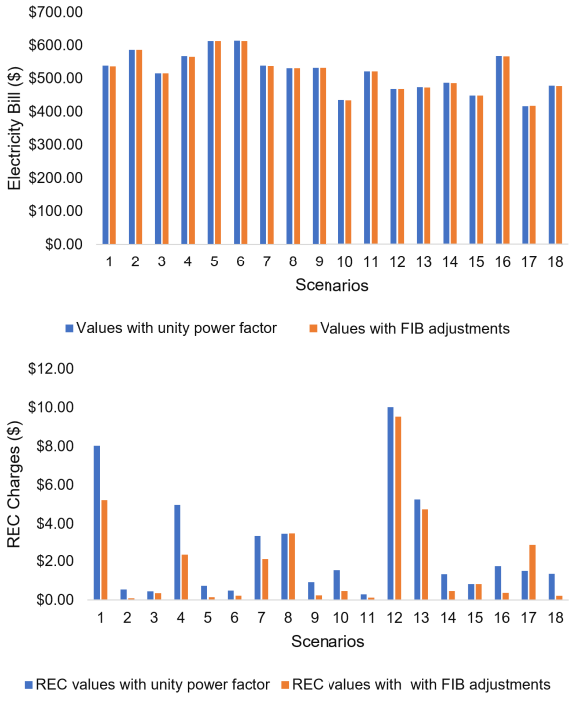

FIGURE 26. Fibonacci - Billing and REC costs for the UFABC consumer($\sigma_{ref} = 0.95$).

Fig. 23 to 26 show that the Fibonacci Search approach reduced the objective function in 17 of those scenarios.

B. INDUSTRIAL LOAD PROFILE

This section presents the results for the industrial load profile using the FPA, PSO, and Fibonacci Search algorithms, along with varying σ_{ref} values.

1) CONFIDENCE INTERVALS

For the industrial consumer load profile, setting the minimum power factor to 0.85 resulted in no penalties, as no violations were detected. At a threshold of 0.9, penalties occurred in 16 of the 18 scenarios, with a maximum of 14 violations observed between 6 AM and 6 PM. At thresholds of 0.92 and 0.95, penalties were present in all scenarios. Specifically, with a threshold of 0.92, the maximum number of infractions increased to 16, and at 0.95, it reached 18.

Tables 23 and 24 display the confidence intervals obtained by varying the power factor using the FPA technique. With FPA, no PV inverters maintained a unity power factor during any violations.

TABLE 23. FPA - Power factor adjustment C.I of the PV inverters for industrial consumer ($\sigma_{ref} = 0.9$).

PV Code	Min. Limit f_p value	Max. Limit f_p value	Mean value
PV 01	0.93	0.96	0.95
PV 02	0.94	0.97	0.95
PV 03	0.93	0.96	0.95
PV 04	0.93	0.97	0.95
PV 05	0.94	0.97	0.95
PV 06	0.93	0.97	0.95
PV 07	0.94	0.96	0.95
PV 08	0.94	0.97	0.95
PV 09	0.94	0.97	0.95

TABLE 24. FPA - Power factor adjustment C.I of the PV inverters for industrial consumer ($\sigma_{ref} = 0.95$).

PV Code	Min. Limit f_p value	Max. Limit f_p value	Mean value
PV 01	0.93	0.96	0.95
PV 02	0.93	0.96	0.95
PV 03	0.93	0.96	0.95
PV 04	0.94	0.95	0.95
PV 05	0.94	0.96	0.95
PV 06	0.93	0.96	0.95
PV 07	0.94	0.96	0.95
PV 08	0.93	0.96	0.95
PV 09	0.94	0.97	0.95

Table 25 and 18 provide the results obtained using the PSO technique. Similar to FPA, PSO did not maintain any PV inverter at a unity power factor when violations occurred.

Tables 28 to 30 show the results using the Fibonacci Search algorithm. This algorithm makes minimal adjustments to power factor values. For example, when targeting a standard power factor of 0.92, inverters 7, 8, and 9 consistently remain at a unity power factor.

TABLE 25. PSO - Power factor adjustment C.I of the PV inverters for industrial consumer ($\sigma_{ref} = 0.9$).

PV Code	Min. Limit f_p value	Max. Limit f_p value	Mean value
PV 01	0.93	0.96	0.95
PV 02	0.94	0.97	0.95
PV 03	0.94	0.97	0.95
PV 04	0.94	0.97	0.95
PV 05	0.94	0.97	0.95
PV 06	0.93	0.96	0.95
PV 07	0.94	0.97	0.95
PV 08	0.93	0.96	0.95
PV 09	0.93	0.96	0.95

TABLE 26. PSO - Power factor adjustment C.I of the PV inverters for industrial consumer ($\sigma_{ref} = 0.92$).

PV Code	Min. Limit f_p value	Max. Limit f_p value	Mean value
PV 01	0.92	0.96	0.93
PV 02	0.93	0.97	0.92
PV 03	0.93	0.97	0.93
PV 04	0.93	0.97	0.98
PV 05	0.93	0.98	0.95
PV 06	0.93	0.97	0.92
PV 07	0.92	0.96	0.94
PV 08	0.93	0.98	0.91
PV 09	0.93	0.96	0.92

TABLE 27. PSO - Power factor adjustment C.I of the PV inverters for industrial consumer ($\sigma_{ref} = 0.95$).

PV Code	Min. Limit f_p value	Max. Limit f_p value	Mean value
PV 01	0.94	0.96	0.95
PV 02	0.93	0.96	0.95
PV 03	0.94	0.97	0.95
PV 04	0.93	0.96	0.95
PV 05	0.93	0.96	0.95
PV 06	0.93	0.96	0.95
PV 07	0.93	0.96	0.95
PV 08	0.93	0.96	0.95
PV 09	0.94	0.97	0.92

TABLE 28. Fibonacci - Power factor adjustment C.I of the PV inverters for industrial consumer ($\sigma_{ref} = 0.9$).

PV Code	Min. Limit f_p value	Max. Limit f_p value	Mean value
PV 01	0.95	0.98	0.97
PV 02	0.91	0.96	0.94
PV 03	0.98	1.00	0.99
PV 04	1.00	1.00	1.00
PV 05	1.00	1.00	1.00
PV 06	1.00	1.00	1.00
PV 07	1.00	1.00	1.00
PV 08	1.00	1.00	1.00
PV 09	1.00	1.00	1.00

2) BILLING AND REC COSTS

Figs. 27, 28 present billing and REC costs using the FPA technique.

TABLE 29. Fibonacci - Power factor adjustment C.I of the PV inverters for industrial consumer ($\sigma_{ref} = 0.92$).

PV Code	Min. Limit f_p value	Max. Limit f_p value	Mean value
PV 01	0.93	0.97	0.95
PV 02	0.91	0.96	0.94
PV 03	0.95	0.99	0.97
PV 04	0.94	0.99	0.96
PV 05	0.98	1.00	0.99
PV 06	1.00	1.00	1.00
PV 07	1.00	1.00	1.00
PV 08	1.00	1.00	1.00
PV 09	1.00	1.00	1.00

TABLE 30. Fibonacci - Power factor adjustment C.I of the PV inverters for industrial consumer ($\sigma_{ref} = 0.95$).

PV Code	Min. Limit f_p value	Max. Limit f_p value	Mean value
PV 01	0.90	0.94	0.92
PV 02	0.90	0.94	0.92
PV 03	0.90	0.94	0.92
PV 04	0.90	0.94	0.92
PV 05	0.90	0.94	0.92
PV 06	0.90	0.94	0.92
PV 07	0.90	0.94	0.92
PV 08	0.91	0.95	0.93
PV 09	0.91	0.96	0.94

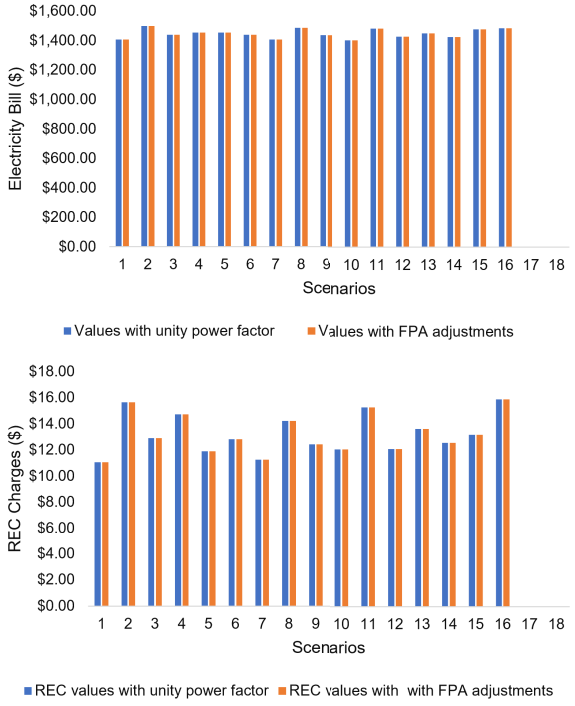

FIGURE 27. FPA - Billing and REC costs for the industrial consumer ($\sigma_{ref} = 0.9$).

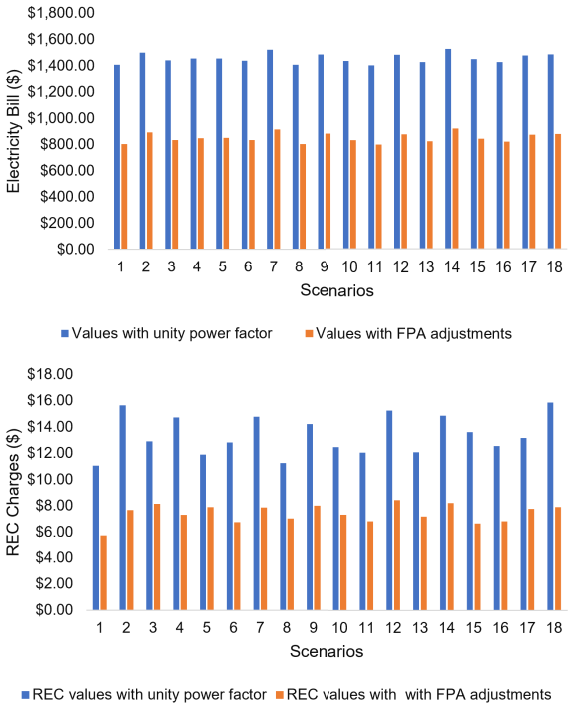

FIGURE 28. FPA - Billing and REC costs for the industrial consumer ($\sigma_{ref} = 0.95$).

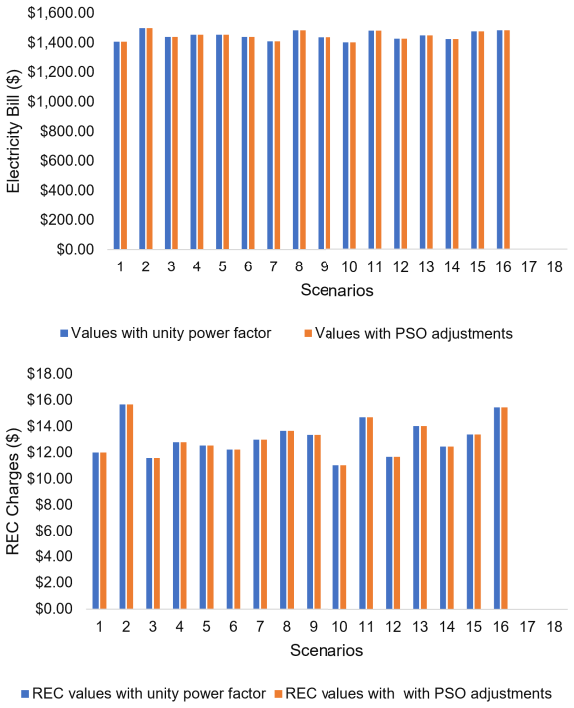

FIGURE 29. PSO - Billing and REC costs for the industrial consumer ($\sigma_{ref} = 0.9$).

The FPA technique delivers results that reduce the objective function in all 18 scenarios. The results obtained using the PSO technique are provided in Figs. 29, 30 and 31.

The objective function is reduced in 10 scenarios. It is important to note that, as a metaheuristic, the quality of the

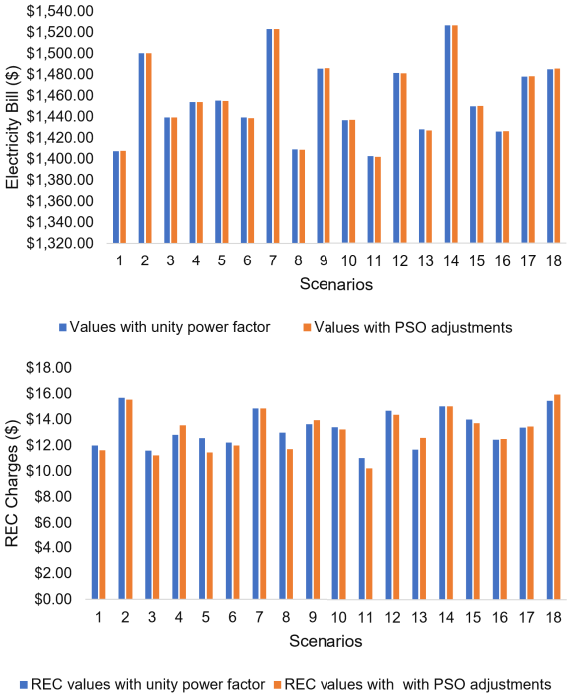

FIGURE 30. PSO - Billing and REC costs for the industrial consumer ($\sigma_{ref} = 0.92$).

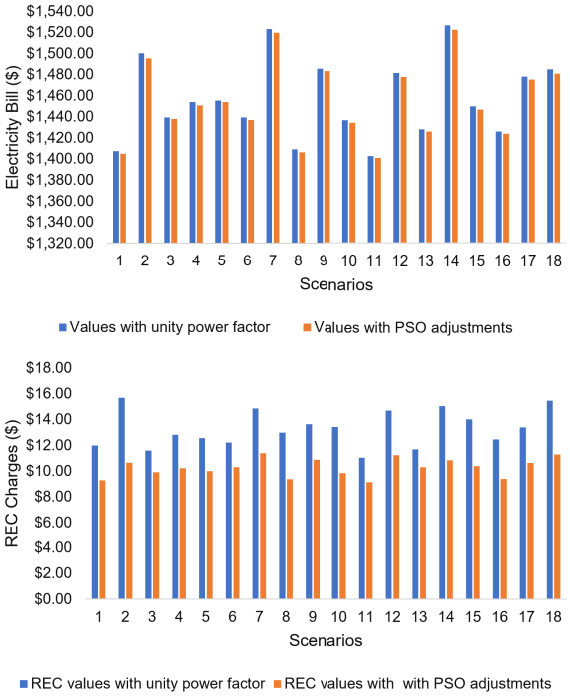

FIGURE 31. PSO - Billing and REC costs for the industrial consumer ($\sigma_{ref} = 0.95$).

FIGURE 32. Fibonacci - Billing and REC costs for the industrial consumer ($\sigma_{ref} = 0.9$).

FIGURE 33. Fibonacci - Billing and REC costs for the industrial consumer ($\sigma_{ref} = 0.92$).

results (evaluated based on the reduction in the objective function) may vary with different runs of the algorithm. Similarly, Figs. 32, 33, and 34 display the results using the Fibonacci Search algorithm.

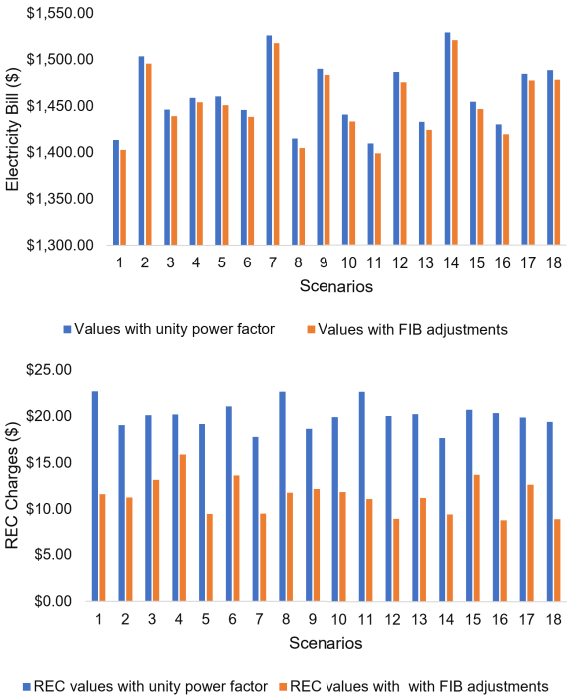

FIGURE 34. Fibonacci - Billing and REC costs for the Industrial Consumer ($\sigma_{ref} = 0.95$).

For the industrial consumer, the objective function was minimized in all 18 scenarios.

REFERENCES

[1] G. Aquila, E. D. O. Pamplona, A. R. D. Queiroz, P. Rotela Jr., and M. N. Fonseca, "An overview of incentive policies for the expansion of renewable energy generation in electricity power systems and the Brazilian experience," *Renew. Sustain. Energy Rev.*, vol. 70, pp. 1090–1098, Apr. 2017, doi: 10.1016/j.rser.2016.12.013.

[2] M. Emmanuel and Y. Zhang, "Estimating spatial distribution impacts of rooftops solar PV on dynamic hosting capacity evaluation for a real distribution feeder," in *Proc. IEEE 48th Photovoltaic Spec. Conf. (PVSC)*, Jun. 2021, pp. 1565–1569.

[3] ABSOLAR. (2024). *Panorama Da Solar Fotovoltaica No Brazil E No Mundo*. [Online]. Available: https://tinyurl.com/yelslb5u

[4] ONS. (2024). *Historico Da Operação*. [Online]. Available: https://tinyurl.com/2az6a2v3

[5] S. M. Ismael, S. H. E. A. Aleem, A. Y. Abdelaziz, and A. F. Zobaa, "State-of-the-art of hosting capacity in modern power systems with distributed generation," *Renew. Energy*, vol. 130, pp. 1002–1020, Jan. 2019, doi: 10.1016/j.renene.2018.07.008.

[6] T. Aziz and N. Ketjoy, "PV penetration limits in low voltage networks and voltage variations," *IEEE Access*, vol. 5, pp. 16784–16792, 2017. [Online]. Available: https://tinyurl.com/27mfycxn

[7] S. K. Sahu and D. Ghosh, "Hosting capacity enhancement in distribution system in highly trenchant photo-voltaic environment: A hardware in loop approach," *IEEE Access*, vol. 8, pp. 14440–14451, 2020.

[8] R. Tonkoski, D. Turcotte, and T. H. M. EL-Fouly, "Impact of high PV penetration on voltage profiles in residential neighborhoods," *IEEE Trans. Sustain. Energy*, vol. 3, no. 3, pp. 518–527, Jul. 2012.

[9] A. Spring, G. Wirth, G. Becker, R. Pardatscher, and R. Witzmann, "Grid influences from reactive power flow of photovoltaic inverters with a power factor specification of one," *IEEE Trans. Smart Grid*, vol. 7, no. 3, pp. 1222–1229, May 2016.

[10] R. da Silva Benedito, R. Zilles, and J. T. Pinho, "Overcoming the power factor apparent degradation of loads fed by photovoltaic distributed generators," *Renew. Energy*, vol. 164, pp. 1364–1375, Feb. 2021, doi: 10.1016/j.renene.2020.10.146.

[11] L. S. Gusman, H. A. Pereira, J. M. S. Callegari, and A. F. Cupertino, "Design for reliability of multifunctional PV inverters used in industrial power factor regulation," *Int. J. Electr. Power Energy Syst.*, vol. 119, Jul. 2020, Art. no. 105932, doi: 10.1016/j.ijepes.2020.105932.

[12] ENERGY. (2022). *Planning a Home Solar Electric System*. [Online]. Available: https://tinyurl.com/yb884bou

[13] SMA. (2022). *Penalty for Reactive Power Consumption or Low Power Factor When Solar is Connected*. [Online]. Available: https://tinyurl.com/262b4lx4

[14] M. U. Hashmi, D. Deka, A. Busic, L. Pereira, and S. Backhaus, "Arbitrage with power factor correction using energy storage," *IEEE Trans. Power Syst.*, vol. 35, no. 4, pp. 2693–2703, Jul. 2020.

[15] ANEEL, "Resolução normativa ANEEL N° 1.000, de 7 de Dezembro de 2021," ANEEL, Nat. Electr. Energy Agency, Brasilia, Brazil, Tech. Rep. 1000, 2021. [Online]. Available: https://tinyurl.com/2lbjkohu

[16] D. Power. (2022). *Reactive Power*. [Online]. Available: https://directpower.co.uk/reactive-power

[17] Essential Services Commission. (2023). *Electricity Distribution Code of Practice*. [Online]. Available: https://tinyurl.com/27nsalov

[18] Office of the Tasmanian Economic Regulator (OTTER), "Distribution system operation Tasmanian," in *Tasmanian Electricity Code Version*. Mountain View, CA, USA: OTTER, Apr. 2021, ch. 8, pp. 257–283. [Online]. Available: https://tinyurl.com/24wdmxy8

[19] TNB. (2024). *FAQ*. [Online]. Available: https://www.tnb.com.my/faq/icpt-english/

[20] TNB. (2022). *Charges and Penalties*. [Online]. Available: https://tinyurl.com/2af854hl

[21] ENTSO-E. (2020). *European Network of Transmission System Operators for Electricity About ENTSO-E*. [Online]. Available: https://tinyurl.com/ywxouhkw

[22] ONS, "Requisitos mínimos para o Sistema de Medição para Faturamento," ONS, Nat. Electr. Syst. Operator (ONS), Brasilia, Brazil, Tech. Rep., Dec. 2020. [Online]. Available: https://tinyurl.com/28d2jfup

[23] ANEEL, "Resolução normativa N° 846, de 11 de Junho de 2019," ANEEL, Nat. Electr. Energy Agency, Brasilia, Brazil, Tech. Rep. 846, 2019. [Online]. Available: https://tinyurl.com/2279mjky

[24] D. D. M. S. B. Lutovac, "Technical assistance for the connection network codes implementation in the energy community," Electr. Coordinating Center Ltd., Vienna, Austria, Tech. Rep. 062021, 2021. [Online]. Available: www.energy-community.org

[25] J. P. Ram, D. S. Pillai, A. M. Ghias, and N. Rajasekar, "Performance enhancement of solar pv systems applying P&O assisted flower pollination algorithm (FPA)," *Sol. Energy*, vol. 199, pp. 214–229, Jan. 2020. [Online]. Available: https://tinyurl.com/23vlfs86

[26] F. D. Murdianto, A. R. Nansur, and A. S. L. Hermawan, "Modeling and simulation of MPPT coupled inductor Sepie converter using flower pollination algorithm (FPA) method in DC mierogrid system," in *Proc. Int. Electron. Symp. Eng. Technol. Appl. (IES-ETA)*, Sep. 2017, pp. 7–13.

[27] S. Suyanto, L. Mohammad, I. C. Setiadi, and R. Roekmono, "Analysis and evaluation performance of MPPT algorithms: Perturb & observe (P&O), firefly, and flower pollination (FPA) in smart microgrid solar panel systems," in *Proc. Int. Conf. Technol. Policies Electr. Power & Energy*, Oct. 2019, pp. 1–6.

[28] X.-S. Yang, "Flower pollination algorithm for global optimization," in *Unconventional Computation and Natural Computation*, J. Durand-Lose and N. Jonoska, Eds., Berlin, Germany: Springer, 2012, pp. 240–249.

[29] R. C. Dugan and D. Montenegro, "Reference guide the open distribution system simulator (OpenDSS)," EPRI, Tech. Rep., 2020. [Online]. Available: https://tinyurl.com/2yd27xcd

[30] R. D. Zimmerman and C. E. Murillo-s. (2020). *Matpower User's Manual Version 7.1*. [Online]. Available: https://matpower.org/doc/

[31] Richard Lincoln. (2011). *Pypower Documentation 4.0.1*. [Online]. Available: https://pypi.org/project/PYPOWER/4.0.1/

[32] T. Alquthami, R. S. Kumar, and A. A. Shaikh, "Mitigation of voltage rise due to high solar PV penetration in Saudi distribution network," *Electr. Eng.*, vol. 102, no. 2, pp. 881–890, Jun. 2020.

[33] M. Karimi, H. Mokhlis, K. Naidu, S. Uddin, and A. H. A. Bakar, "Photovoltaic penetration issues and impacts in distribution network—A review," *Renew. Sustain. Energy Rev.*, vol. 53, pp. 594–605, Jan. 2016.

[34] M. Ebad and W. M. Grady, "An approach for assessing high-penetration PV impact on distribution feeders," *Electr. Power Syst. Res.*, vol. 133, pp. 347–354, Apr. 2016.

[35] P. Radatz. (2022). *Py-Dss-Interface User's Manual*. [Online]. Available: https://pypi.org/project/py-dss-interface/

[36] Banco Central do Brasil. (2023). *Boletim Focus*. Março. [Online]. Available: https://encurtador.com.br/flGJZ
[37] J. T. Pinho and M. A. Galdino, *Manual de Engenharia Para Sistemas Fotovoltaicos*, document CEPL-CRESESB, 2014.
[38] A. Hayes. (2022). *What Is a Confidence Interval and How Do You Calculate It*. [Online]. Available: https://t.ly/qGN6
[39] B. U. S. O. P. Health. (2021). *Confidence Intervals for Sample Size Less Than 30*. [Online]. Available: https://tinyurl.com/2eqoa64e
[40] V. Sharma, S. M. Aziz, M. H. Haque, and T. Kauschke, "Effects of high solar photovoltaic penetration on distribution feeders and the economic impact," *Renew. Sustain. Energy Rev.*, vol. 131, Oct. 2020, Art. no. 110021, doi: 10.1016/j.rser.2020.110021.
[41] D. Cheng, B. A. Mather, R. Seguin, J. Hambrick, and R. P. Broadwater, "Photovoltaic (PV) impact assessment for very high penetration levels," *IEEE J. Photovolt.*, vol. 6, no. 1, pp. 295–300, Jan. 2016, doi: 10.1109/JPHOTOV.2015.2481605.
[42] J. V. Gastelu, V. G. Borges, and J. D. M. Trujillo, "Photovoltaic potential spatial estimation considering shading effects," in *Proc. IEEE PES Innov. Smart Grid Technol. Conf. Latin Amer. (ISGT Latin Amer.)*, Sep. 2021, pp. 1–5.
[43] E. D. S. Paulo, "Relatório da administração 2021," ENEL Distribuição Paulo, Sao Paulo, Brazil, Tech. Rep., Dec. 2021. [Online]. Available: https://tinyurl.com/2bk27yat
[44] C. E. M. Rodrigues, M. E. de Lima Tostes, U. H. Bezerra, T. M. Soares, E. O. de Matos, L. S. S. Filho, E. C. dos Santos Silva, M. F. Rendeiro, and C. J. da Silva Moura, "Technical loss calculation in distribution grids using equivalent minimum order networks and an iterative power factor correction procedure," *Energies*, vol. 14, no. 3, p. 646, Jan. 2021.
[45] T. T. Nguyen, B. H. Dinh, T. D. Pham, and T. T. Nguyen, "Active power loss reduction for radial distribution systems by placing capacitors and PV systems with geography location constraints," *Sustainability*, vol. 12, no. 18, p. 7806, Sep. 2020.
[46] T. Das, R. Roy, and K. K. Mandal, "Impact of the penetration of distributed generation on optimal reactive power dispatch," *Protection Control Modern Power Syst.*, vol. 5, no. 1, pp. 1–26, Dec. 2020.

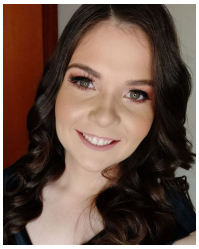

DARLENE J. DULLIUS received the B.S. degree in electrical engineering from the Federal University of Tocantins, Palmas, Brazil, in 2019, and the M.Sc. degree in electrical engineering from the Federal University of ABC, Santo André, Brazil, in 2022, where she is currently pursuing the Ph.D. degree in energy. Her research interests include power network modernization and operation.

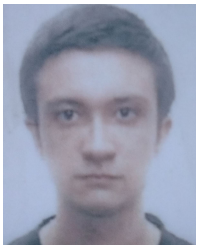

VICTOR GABRIEL BORGES received the B.S. degree in Science and Technology from the Federal University of ABC, Santo André, Brazil, in 2022, where he is currently pursuing the M.Sc. degree in energy. His current research interests include power network planning and spatial analysis.

RENZO VARGAS received the B.S. degree in electrical engineering from the National University of Engineering, Lima, Peru, in 2012, and the M.S. and Ph.D. degrees in electrical engineering from São Paulo State University (UNESP), Ilha Solteira, Brazil, in 2015 and 2019, respectively.

He is currently a Postdoctoral Researcher with São Paulo State University. His current research interests include the development of methods for the optimization, planning, and control of electrical power systems.

CAITLIN GUSK received the B.S. degree in electrical engineering from the Milwaukee School of Engineering, in 2015, and the M.E. degree in power systems engineering from Worcester Polytechnic Institute, in 2022. She is currently pursuing the Ph.D. degree with the University of Maine.

She was a Distribution Engineer with Versant Power. She is currently a Project Engineer I with Electrical Consultants, Inc. Her research interests include grid reliability and resiliency, grid modernization, and the effect the modern grid may have on consumers.

REINALDO TONKOSKI (Senior Member, IEEE) received the B.A.Sc. degree in control and automation engineering and the M.Sc. degree in electrical engineering from the Pontifícia Universidade Católica do Rio Grande do Sul (PUC-RS), Brazil, in 2004 and 2006, respectively, and the Ph.D. degree from Concordia University, Canada, in 2011.

He is currently a Professor and the Head of the Chair of the Electric Power Transmission and Distribution, Technical University of Munich. He has authored over one hundred technical publications in peer-reviewed journals and conferences and is also an Editor of IEEE TRANSACTIONS ON SUSTAINABLE ENERGY, IEEE ACCESS, and IEEE SYSTEMS JOURNAL. His research interests include grid integration of sustainable energy technologies, energy management, power electronics, and control systems.

JOEL D. MELO (Senior Member, IEEE) received the B.S. degree in electrical engineering from UNMSM, Lima, Peru, in 2006, and the M.Sc. and Ph.D. degrees in electrical engineering from UNESP, Ilha Solteira, Brazil, in 2010 and 2014, respectively. He is currently an Associate Professor with the Federal University of ABC (UFABC), participating in developing research projects for electrical utilities. His research interests include power network planning and spatial analysis.

MAHDI POURAKBARI KASMAEI (Senior Member, IEEE) received the Ph.D. degree in electrical power engineering from São Paulo State University (UNESP), Ilha Solteira, Brazil, in 2015. He was a Postdoctoral Fellow with UNESP and also a Visiting Researcher with the University of Castilla-La Mancha, Spain. He is currently an Assistant Professor with the Department of Electrical Engineering and Automation, Aalto University, Finland, where he used to be a Postdoctoral Researcher. He is responsible for the "electric energy and hydrogen systems" major at Aalto University and the Leader of the Power and Energy Systems Group. He was a project executive or principal investigator of several practical and academic projects and also a consultant in an electric power distribution company. His research interests include power and energy systems planning, operations, economics, environmental issues, multi-energy sector dynamics, as well as power system protection and transients. He is the Chair of the IEEE Finland Section and the IEEE Finland PES&IES (IE13/PE31/34/PEL35) Joint Chapter and an Associate Editor of journals, such as *IET Generation, Transmission and Distribution*, IEEE ACCESS, and *Journal of Control, Automation and Electrical Systems*. He was the Ambassador of Clean Energy in the IEEE Finland Section and the General Chair of the IEEE PES ISGT-Europe 2021 Conference.